A STABLE AND CONVERGENT METHOD FOR HODGE DECOMPOSITION OF FLUID-SOLID INTERACTION

GANGJOON YOON, CHOHONG MIN†, AND SEICK KIM

ABSTRACT. Fluid-solid interaction has been a challenging subject due to their strong nonlinearity and multidisciplinary nature. Many of the numerical methods for solving FSI problems have struggled with non-convergence and numerical instability. In spite of comprehensive studies, it has been still a challenge to develop a method that guarantees both convergence and stability.

Our discussion in this work is restricted to the interaction of viscous incompressible fluid flow and a rigid body. We take the monolithic approach by Gibou and Min [22] that results in an extended Hodge projection. The projection updates not only the fluid vector field but also the solid velocities. We derive the equivalence of the extended Hodge projection to the Poisson equation with non-local Robin boundary condition. We prove the existence, uniqueness, and regularity for the weak solution of the Poisson equation, through which the Hodge projection is shown to be unique and orthogonal. Also, we show the stability of the projection in a sense that the projection does not increase the total kinetic energy of fluid and solid. Also, we discuss a numerical method as a discrete analogue to the Hodge projection, then we show that the unique decomposition and orthogonality also hold in the discrete setting. As one of our main results, we prove that the numerical solution is convergent with at least the first order accuracy. We carry out numerical experiments in two and three dimensions, which validate our analysis and arguments.

1. Introduction

In this article, we consider the interaction of fluid and structure. An immersed structure in fluid interacts with fluid in two ways. On their interface, fluid cannot penetrate into structure and the motion of structure is affected by the normal stress of fluid. Fluid-structure interaction (FSI) has been a challenging subject due to their strong nonlinearity and multidisciplinary nature ([10], [14], [34]). In many scientific and engineering areas, FSI problems play prominent roles, but it is hard or impossible to find exact solutions to the problems, so that their solutions should have been approximated by numerical solutions.

For approximating FSI problems, numerous numerical methods have been proposed. Most of them have struggled with non-convergence ([5], [9], [19], [25]) and numerical instability [41]. Only few of them have guaranteed stability ([6], [22], [24]). In spite of comprehensive studies, it has been still a challenge to develop a method that guarantees both convergence and stability.

There are two main approaches to obtain a numerical method for the FSI problems : Monolithic and partitioned approaches. The monolithic approach treats the fluid and structure dynamics

2000 *Mathematics Subject Classification.* Primary 76D03, 65N06, 76M20; Secondary 35Q30, 35J25.

Key words and phrases. Fluid-solid interaction, Helmholtz-Hodge decomposition, Augmented Hodge decomposition, Numerical analysis.

† Corresponding author. C. Min was supported by Basic Science Research Program through the National Research Foundation of Korea(NRF) funded by the Ministry of Education(2009-0093827).

S. Kim is supported by NRF-20151009350.

in the same mathematical framework, and the partitioned approach treats them separately. The monolithic approach [29, 32, 40, 42] solves simultaneously the linearized equations of fluid-structure coupling conditions in one system. Even though this approach achieves better accuracy for the multidisciplinary problem, usually it requires well-designed preconditioners and costs quite expensive computational time [2, 20, 27]. To reduce the computational time, the partitioned approach treats the structure and the fluid as the two physical fields and solves them separately. Even though the partitioned methods have been extensively studied and developed [1, 8, 13, 16, 37], this approach still requires the construction of efficient schemes to produce stable, accurate results. Despite the recent developments, only a few partitioned methods have guaranteed the convergence [17, 18, 35].

Our discussion is restricted to the interaction of viscous incompressible fluid flow and a rigid body. The incompressible fluid flow is governed by the Navier-Stokes equations and the motion rigid body is governed by the Euler equations. On their interface $\Gamma(t)$, fluid and solid interacts in two ways. They should have the same normal velocity component and fluid delivers the net force of normal stress to solid. Combining the governing equations and taking into consideration the two-way couplings, we have the following two syatems of equations for fluid and solid: consisting of the system of momentum equation and incompressible condition:

$$\begin{cases} \rho(\boldsymbol{U}_t + \boldsymbol{U}\cdot\nabla\boldsymbol{U}) = -\nabla p + \nabla\cdot(2\mu\mathbb{D}) \quad \text{in } \Omega \\ \nabla\cdot\boldsymbol{U} = 0 \quad \text{in } \Omega. \end{cases} \tag{1.1}$$

and

$$\begin{cases} \dot{\boldsymbol{c}} = \boldsymbol{v} \\ m\dot{\boldsymbol{v}} = f \\ \mathbb{I}\dot{\boldsymbol{\omega}} = \tau. \end{cases} \tag{1.2}$$

Here, $\boldsymbol{U}$ is the flow vector field and $\boldsymbol{v}(t)$ and $\boldsymbol{\omega}(t)$ denote the linear and angular velocities at the center of mass $\boldsymbol{c}(t)$ of the rigid body, respectively. With $\boldsymbol{J} := (\boldsymbol{x}-\boldsymbol{c})\times\boldsymbol{n}$, note that $\boldsymbol{U}\cdot\boldsymbol{n} = (\boldsymbol{v}+\boldsymbol{\omega}\times(\boldsymbol{x}-\boldsymbol{c}))\cdot\boldsymbol{n}$ describes the non-penetration boundary condition at the interface. The other notations follow the standard settings and we refer to [22] for more details.

The incompressible condition prevents the development of a discontinuity, and a standard approach to approximate the time derivatives in the system of equations (1.1)and (1.2), and is the second order SL-BDF method [22, 43], which can be written in the followoing two steps. The first step is to solve the system with a pressure guess.

$$\begin{cases} \rho\frac{\frac{3}{2}U^*-2U^n+\frac{1}{2}U^{n-1}}{\Delta t} &=& -\nabla p^n + \nabla\cdot(2\mu\mathbb{D}^*) \text{ in } \Omega^{n+1} \\ \frac{\frac{3}{2}c^*-2c^n+\frac{1}{2}c^{n-1}}{\Delta t} &=& 2v^n - v^{n-1} \\ m\frac{\frac{3}{2}v^*-2v^n+\frac{1}{2}v^{n-1}}{\Delta t} &=& \int_{\Gamma^{n+1}}(p^n-2\mu\mathbb{D}^*)\,n\,ds \\ \mathbb{I}\frac{\frac{3}{2}\omega^*-2\omega^n+\frac{1}{2}\omega^{n-1}}{\Delta t} &=& \int_{\Gamma^{n+1}}\left(x-c^{n+1}\right)\times(p^n-2\mu\mathbb{D}^*)\,n\,ds \end{cases}$$

The second step is basically to enforce the divergence-free condition and impose the two-way coupled interactions.

$$\begin{cases} \rho U^* &=& \rho U^{n+1}+\nabla q^{n+1} & \text{in } \Omega^{n+1} \\ \nabla\cdot U^{n+1} &=& 0 & \text{in } \Omega^{n+1} \\ U^{n+1}\cdot n &=& v^{n+1}\cdot n+\omega^{n+1}\cdot J & \text{in } \Gamma^{n+1} \\ mv^* &=& mv^{n+1}-\int_{\Gamma^{n+1}}q^{n+1}n\,ds \\ \mathbb{I}\omega^* &=& \mathbb{I}\omega^{n+1}-\int_{\Gamma^{n+1}}q^{n+1}J\,ds \end{cases}$$

The conventional Hodge decomposition splits a vector field into a unique sum of the divergence-free vector field and the gradient field. We take the monolithic approach that updates not only the fluid

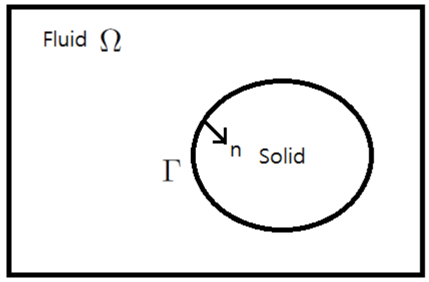

FIGURE 2.1. Fluid-solid interaction

vector field but also the solid velocities. As we shall discuss in details in Section 2, the monolithic extension of the conventional Hodge projection that are denoted by

$$\left(\boldsymbol{U}^{n+1}, \boldsymbol{v}^{n+1}, \boldsymbol{\omega}^{n+1}\right) = \mathcal{P}\left(\boldsymbol{U}^*, \boldsymbol{v}^*, \boldsymbol{\omega}^*\right).$$

We derive the equivalence of the extended Hodge projection to the Poisson equation with non-local Robin boundary condition. In Section 3, we prove the existence, uniqueness, and regularity for the weak solution of the Poisson equation, through which the Hodge projection is shown to be unique and orthogonal. Also, we show the stability of the projection in a sense that the projection does not increase the total kinetic energy of fluid and solid. Section 4 discusses the numerical method [22] as a discrete analogue to the Hodge projection, and shows that the unique decomposition and orthogonality also hold in the discrete setting. In Section 5, we prove that the numerical solution is convergent with at least the first order accuracy. In Section 6, we carry out numerical experiments in two and three dimensions. The numerical tests validate our analysis and arguments.

2. MONOLITHIC DECOMPOSITION

Let $\Omega \subset \mathbb{R}^d$ $(d = 2, 3)$ be a bounded domain (i.e., open connected set) with boundary $\partial\Omega = \Gamma \cup \Gamma'$, where $\Gamma \cap \Gamma' = \emptyset$. We assume that the domain Ω is occupied by an incompressible fluid and Γ is the interface with the fluid and a solid; the other part Γ' of the boundary is always fixed. Assume that a fluid vector field $\boldsymbol{U}^* : \Omega \to \mathbb{R}^d$ and a solid linear velocity $\boldsymbol{v}^* \in \mathbb{R}^d$ and angular velocity $\boldsymbol{\omega}^* \in \mathbb{R}^d$ are given. After the fluid-solid interaction and the incompressible condition applied, the fluid vector field becomes solenoidal and the fluid vector field and solid vector field have the same normal component on the fluid-solid interface Γ.

In this work, we try to decompose $(\boldsymbol{U}^*, \boldsymbol{v}^*, \boldsymbol{\omega}^*)$ as

$$\begin{cases} \rho\boldsymbol{U}^* = \rho\boldsymbol{U} + \nabla p \quad \text{in } \Omega \\ m\boldsymbol{v}^* = m\boldsymbol{v} - \displaystyle\int_\Gamma p\boldsymbol{n}\, dS \\ \mathbb{I}\boldsymbol{\omega}^* = \mathbb{I}\boldsymbol{\omega} - \displaystyle\int_\Gamma p\boldsymbol{J}\, dS \end{cases} \tag{2.1}$$

with a vector field $\boldsymbol{U} : \Omega \to \mathbb{R}^d$ and a scalar field $p : \Omega \to \mathbb{R}$ and velocities $\boldsymbol{v}, \boldsymbol{\omega} \in \mathbb{R}^d$ that satisfy the incompressible condition and the non-penetration condition

$$\begin{cases} \nabla\cdot\boldsymbol{U}=0 \quad \text{in } \Omega \\ \boldsymbol{U}\cdot\boldsymbol{n}=\boldsymbol{v}\cdot\boldsymbol{n}+\boldsymbol{\omega}\cdot\boldsymbol{J} \quad \text{on } \Gamma \\ \boldsymbol{U}\cdot\boldsymbol{n}=0 \quad \text{on } \Gamma'. \end{cases} \tag{2.2}$$

When we find a scalar function p in (2.1), the decomposition is achieved monolithically by setting $(\boldsymbol{U},\boldsymbol{v},\boldsymbol{\omega})$ as

$$(\boldsymbol{U},\boldsymbol{v},\boldsymbol{\omega}):=(\boldsymbol{U}^*,\boldsymbol{v}^*,\boldsymbol{\omega}^*)-\left(\frac{1}{\rho}\nabla p,\ -\frac{1}{m}\int_\Gamma p\boldsymbol{n}\,dS,\ -\mathbb{I}^{-1}\int_\Gamma p\boldsymbol{J}\,dS\right).$$

We call $(\boldsymbol{U},\boldsymbol{v},\boldsymbol{\omega})$ the augmented Hodge projection of the state variable $(\boldsymbol{U}^*,\boldsymbol{v}^*,\boldsymbol{\omega}^*)$,

$$(\boldsymbol{U},\boldsymbol{v},\boldsymbol{\omega})=\mathcal{P}\left(\boldsymbol{U}^*,\boldsymbol{v}^*,\boldsymbol{\omega}^*\right),$$

and we will check the stability of the projection by estimating the kinetic energies and show the orthogonality of the decomposition (2.1) with respect to the inner product induced by the kinetic energy.

The existence and uniqueness of the decomposition will be shown in the following section where we will find p by solving a Poisson equation and study more details on the equation.

Throughout this work, ρ is the fluid density, which is assumed to be constant; m is the mass of a rigid body whose boundary is Γ; $\boldsymbol{c}$ is the center of mass of the rigid body; $\mathbb{I}\in\mathbb{R}^{d\times d}$ is a symmetric positive definite matrix, the inertia tensor of the rigid body. And $\boldsymbol{n}$ is the unit normal vector field of Γ and $\boldsymbol{J}$ is a vector field defined on Γ by $\boldsymbol{J}(\boldsymbol{x})=(\boldsymbol{x}-\boldsymbol{c})\times\boldsymbol{n}$ for $\boldsymbol{x}\in\Gamma$.

In case $d=2$, we regard vectors in $\mathbb{R}^2$ as vectors in $\mathbb{R}^3$ by a trivial extension as follows. The angular velocity $\boldsymbol{\omega}$ reads as $\boldsymbol{\omega}=(0,0,\omega)$, and for $\boldsymbol{a}=(a_1,a_2)$ and $\boldsymbol{b}=(b_1,b_2)$, the cross product of $\boldsymbol{a}$ and $\boldsymbol{b}$ is defined to be a scalar $a_1b_2-a_2b_1$ or the vector on z-axis given by $\boldsymbol{a}\times\boldsymbol{b}=(a_1,a_2,0)\times(b_1,b_2,0)$. In this case, however, the vector calculation is fulfilled based on $\mathbb{R}^2$, which may cause no confusion.

We begin by introducing the following lemma, which plays an essential role in this work.

Lemma 2.1. *In the above setting,* $\int_\Gamma \boldsymbol{n}\,dS=0$ *and* $\int_\Gamma \boldsymbol{J}\,dS=0$.

Proof. Let Ω' be a domain (occupied by a solid) whose boundary is Γ. We apply the Gauss-Green theorem to Ω' and get

$$\begin{aligned}\int_\Gamma \boldsymbol{n}\,dS&=-\int_\Gamma 1\,(-\boldsymbol{n})\;dS=-\int_{\Omega'}(\nabla 1)\,dx=0 \quad \text{and}\\ \int_\Gamma \boldsymbol{J}\,dS&=-\int_\Gamma(\boldsymbol{x}-\boldsymbol{c})\times(-\boldsymbol{n})\;dS=\int_{\Omega'}\nabla\times(\boldsymbol{x}-\boldsymbol{c})\,dx=0.\end{aligned}$$

■

2.1. **Orthogonality and stability.** For a given triple $(\boldsymbol{U}^*,\boldsymbol{v}^*,\boldsymbol{\omega}^*)$ with a fluid vector field $\boldsymbol{U}^*:\Omega\to\mathbb{R}^d$ and a solid linear velocity $\boldsymbol{v}^*\in\mathbb{R}^d$ and an angular velocity $\boldsymbol{\omega}^*\in\mathbb{R}^d$, the kinetic energy E^* is given as

$$E^*=\int_\Omega \frac{1}{2}\rho\,|\boldsymbol{U}^*|^2\,dx+\frac{1}{2}m|\boldsymbol{v}^*|^2+\frac{1}{2}\boldsymbol{\omega}^*\cdot\mathbb{I}\boldsymbol{\omega}^*.$$

Let $(\boldsymbol{U},\boldsymbol{v},\boldsymbol{\omega})$ and p be as in the decomposition (2.1) of $(\boldsymbol{U}^*,\boldsymbol{v}^*,\boldsymbol{\omega}^*)$ and let E the energy induced by the triple $(\boldsymbol{U},\boldsymbol{v},\boldsymbol{\omega})$, which is given as

$$E=\int_\Omega \frac{1}{2}\rho\,|\boldsymbol{U}|^2\,dx+\frac{1}{2}m|\boldsymbol{v}|^2+\frac{1}{2}\boldsymbol{\omega}\cdot\mathbb{I}\boldsymbol{\omega}.$$

Now, we estimate the energies E^* and E. Applying the decomposition (2.1), we have

$$
\begin{aligned}
E^* &= \int_\Omega \frac{1}{2}\rho \left|\boldsymbol{U} + \rho^{-1}\nabla p\right|^2 \, dx + \frac{1}{2} m \left| \boldsymbol{v} - \frac{1}{m}\int_\Gamma p\boldsymbol{n}\, dS\right|^2 \\
&\qquad + \frac{1}{2}\left(\boldsymbol{\omega} - \mathbb{I}^{-1}\int_\Gamma p\boldsymbol{J}\, dS\right)\cdot \mathbb{I}\left(\boldsymbol{\omega} - \mathbb{I}^{-1}\int_\Gamma p\boldsymbol{J}\, dS\right) \\
&= \int_\Omega \frac{1}{2}\rho|\boldsymbol{U}|^2\, dx + \frac{1}{2}m|\boldsymbol{v}|^2 + \frac{1}{2}\boldsymbol{\omega}\cdot\mathbb{I}\boldsymbol{\omega} \\
&\qquad + \int_\Omega \boldsymbol{U}\cdot\nabla p\, dx - \boldsymbol{v}\cdot\int_\Gamma p\boldsymbol{n}\, dS - \boldsymbol{\omega}\cdot\int_\Gamma p\boldsymbol{J}\, dS \\
&\qquad + \int_\Omega \frac{1}{2\rho}\left|\nabla p\right|^2 dx + \frac{1}{2m}\left|\int_\Gamma p\boldsymbol{n}\, dS\right|^2 + \frac{1}{2}\left(\mathbb{I}^{-1}\int_\Gamma p\boldsymbol{J}\, dS\right)\cdot\left(\int_\Gamma p\boldsymbol{J}\, dS\right) \\
&\ge \int_\Omega \frac{1}{2}\rho|\boldsymbol{U}|^2\, dx + \frac{1}{2}m|\boldsymbol{v}|^2 + \frac{1}{2}\boldsymbol{\omega}\cdot\mathbb{I}\boldsymbol{\omega} = E.
\end{aligned}
$$

In the above, we used the symmetric positive definiteness of $\mathbb{I}$ and the incompressible and the non-penetration conditions (2.2) which imply

$$
\begin{aligned}
(2.3)\quad \int_\Omega \boldsymbol{U}\cdot\nabla p\, dx - \boldsymbol{v}\cdot\int_\Gamma p\boldsymbol{n}\, dS - \boldsymbol{\omega}\cdot\int_\Gamma p\boldsymbol{J}\, dS &= -\int_\Omega (\nabla\cdot\boldsymbol{U})\, p\, dx \\
+ \int_{\Gamma'} p\boldsymbol{U}\cdot\boldsymbol{n}\, dS + \int_\Gamma p\boldsymbol{U}\cdot\boldsymbol{n}\, dS - \int_\Gamma p\boldsymbol{v}\cdot\boldsymbol{n}\, dS &- \int_\Gamma p\omega\cdot\boldsymbol{J}\, dS = 0.
\end{aligned}
$$

Equation (2.3) implies that the decomposition is orthogonal with respect to the inner product $\langle\cdot,\cdot\rangle_E$ on $L^2(\Omega)^d\times\mathbb{R}^d\times\mathbb{R}^d$ defined by

$$
\begin{aligned}
(2.4)\quad &\big\langle(\boldsymbol{U}^{(1)},\boldsymbol{v}^{(1)},\boldsymbol{\omega}^{(1)}),(\boldsymbol{U}^{(2)},\boldsymbol{v}^{(2)},\boldsymbol{\omega}^{(2)})\big\rangle_E \\
&\qquad := \int_\Omega \frac{1}{2}\rho\, \boldsymbol{U}^{(1)}\cdot\boldsymbol{U}^{(2)}\, dx + \frac{1}{2}m\boldsymbol{v}^{(1)}\cdot\boldsymbol{v}^{(2)} + \frac{1}{2}\boldsymbol{\omega}^{(1)}\cdot\mathbb{I}\boldsymbol{\omega}^{(2)}.
\end{aligned}
$$

We can write the energy E of a triple $(\boldsymbol{U},\boldsymbol{v},\boldsymbol{\omega})$ in terms of the inner product as

$$
E = \int_\Omega \frac{1}{2}\rho\,|\boldsymbol{U}|^2\, dx + \frac{1}{2}m|\boldsymbol{v}|^2 + \frac{1}{2}\boldsymbol{\omega}\cdot\mathbb{I}\boldsymbol{\omega} = \big\langle(\boldsymbol{U},\boldsymbol{v},\boldsymbol{\omega}),(\boldsymbol{U},\boldsymbol{v},\boldsymbol{\omega})\big\rangle_E.
$$

Consequently, we have shown that the projection $(\boldsymbol{U},\boldsymbol{v},\boldsymbol{\omega}) = \mathcal{P}\left(\boldsymbol{U}^*,\boldsymbol{v}^*,\boldsymbol{\omega}^*\right)$, is stable as the kinetic energy E of the projection does not increase comparing with the energy E^* of the state variable. In summary, we have the following:

Theorem 2.1. *For a given triple $(\boldsymbol{U}^*,\boldsymbol{v}^*,\boldsymbol{\omega}^*)$, let the triple $(\boldsymbol{U},\boldsymbol{v},\boldsymbol{\omega})$ be given by*

$$
(2.5)\qquad \Big(\boldsymbol{U}^*,\boldsymbol{v}^*,\boldsymbol{\omega}^*\Big) = \Big(\boldsymbol{U},\boldsymbol{v},\boldsymbol{\omega}\Big) + \left(\frac{1}{\rho}\nabla p, -\frac{1}{m}\int_\Gamma p\boldsymbol{n}\, dS, -\mathbb{I}^{-1}\int_\Gamma p\boldsymbol{J}\, dS\right)
$$

for some scalar function p. If $(\boldsymbol{U},\boldsymbol{v},\boldsymbol{\omega})$ satisfies the conditions

$$
\begin{cases}
\nabla\cdot\boldsymbol{U} = 0 \quad \text{in } \Omega \\
\boldsymbol{U}\cdot\boldsymbol{n} = \boldsymbol{v}\cdot\boldsymbol{n} + \boldsymbol{\omega}\cdot\boldsymbol{J} \quad \text{on } \Gamma, \\
\boldsymbol{U}\cdot\boldsymbol{n} = 0 \quad \text{on } \Gamma'.
\end{cases}
$$

then the decomposition (2.5) *is orthogonal with respect to the inner product* (2.4)*. Furthermore, the kinetic energy decreases in the sense* $E^* \geq E$*.*

3. Poisson equation with nonlocal Robin boundary condition

Taking into account all relations in terms of a scalar field p, the decomposition (2.1) is fulfilled by solving the Poisson equation with nonlocal Robin boundary condition:

$$\begin{cases} -\nabla \cdot \left(\dfrac{1}{\rho}\nabla p\right) = -\nabla \cdot \boldsymbol{U}^* \text{ in } \Omega, \\ \dfrac{1}{\rho}\dfrac{\partial p}{\partial n} + \boldsymbol{n} \cdot \dfrac{1}{m}\displaystyle\int_\Gamma p\boldsymbol{n}\, dS + \boldsymbol{J} \cdot \mathbb{I}^{-1}\int_\Gamma p\boldsymbol{J}\, dS = \boldsymbol{U}^* \cdot \boldsymbol{n} - \boldsymbol{v}^* \cdot \boldsymbol{n} - \boldsymbol{\omega}^* \cdot \boldsymbol{J} \text{ on } \Gamma, \\ \dfrac{1}{\rho}\dfrac{\partial p}{\partial n} = \boldsymbol{U}^* \cdot \boldsymbol{n} \text{ on } \Gamma'. \end{cases} \tag{3.1}$$

In this section, we estimate the existence, uniqueness, and regularity of a solution p to the Poisson equation.

3.1. **Existence and uniqueness.** We will show the existence of a pressure p appearing in the decomposition (2.1) - (2.2) as a weak solution of a Poisson problem with a nonlocal Robin boundary condition; once p is obtained, we compute $(\boldsymbol{U}, \boldsymbol{v}, \boldsymbol{\omega})$ by the formula (2.1).

For the sake of generality and to address regularity issue, we consider the following more general setting: Let $\Omega \subset \mathbb{R}^d$ be a bounded domain with boundary $\partial\Omega$ decomposed into two disjoint parts $\partial\Omega = \Gamma \cup \Gamma'$. For $f \in L^2(\Omega)$, $\boldsymbol{F} \in L^2(\Omega; \mathbb{R}^d)$, and $g \in L^2(\partial\Omega) = L^2(\Gamma \cup \Gamma')$, we consider the following problem

$$-\nabla \cdot (\mathbb{A}\nabla u) = f - \nabla \cdot \boldsymbol{F} \text{ in } \Omega, \tag{3.2}$$

$$\mathbb{A}\nabla u \cdot \boldsymbol{n} = \boldsymbol{F} \cdot \boldsymbol{n} + g \text{ on } \Gamma', \tag{3.3}$$

$$\mathbb{A}\nabla u \cdot \boldsymbol{n} + \left[\alpha \int_\Gamma u\boldsymbol{n}\, dS + \left(\mathbb{B}\int_\Gamma u\boldsymbol{r} \times \boldsymbol{n}\, dS\right) \times \boldsymbol{r}\right] \cdot \boldsymbol{n} = \boldsymbol{F} \cdot \boldsymbol{n} + g \text{ on } \Gamma. \tag{3.4}$$

Here, $\mathbb{A}$ is a symmetric $d \times d$ matrix valued measurable function on $\overline{\Omega}$ satisfying the uniform ellipticity condition; i.e., there are constants $0 < \lambda \leq \Lambda < +\infty$ such that

$$\lambda|\boldsymbol{\xi}|^2 \leq \mathbb{A}(x)\boldsymbol{\xi} \cdot \boldsymbol{\xi} \leq \Lambda|\boldsymbol{\xi}|^2, \quad \forall x \in \overline{\Omega}, \ \forall \boldsymbol{\xi} \in \mathbb{R}^d, \tag{3.5}$$

α is a nonnegative constant, $\mathbb{B}$ is a symmetric nonnegative definite $d \times d$ constant matrix, and $\boldsymbol{r} : \Gamma \to \mathbb{R}^d$ is a bounded vector field satisfying $\int_\Gamma \boldsymbol{r} \times \boldsymbol{n}\, dS = 0$.

Theorem 3.1. *Assume the above conditions. Then the problem* (3.2) – (3.4) *has a weak solution* $u \in H^1(\Omega)$ *if and only if* f *and* g *satisfy the compatibility condition*

$$\int_\Omega f\, dx + \int_{\partial\Omega} g\, dS = 0. \tag{3.6}$$

Moreover, such a weak solution u *is unique modulo an additive constant. In particular, one may assume that* $\int_\Omega u = 0$*.*

Proof. Let us first formulate the problem (3.2) – (3.4) in a weak setting. We multiply (3.2) by a function $v \in H^1(\Omega)$ and integrate by parts on Ω to obtain

$$\int_\Omega \mathbb{A}\nabla u \cdot \nabla v\, dx = \int_{\partial\Omega} (\mathbb{A}\nabla u \cdot \boldsymbol{n} - \boldsymbol{F} \cdot \boldsymbol{n})v\, dS + \int_\Omega fv\, dx + \int_\Omega \boldsymbol{F} \cdot \nabla v\, dx.$$

The boundary conditions (3.3), (3.4), and the vector identity $\boldsymbol{a}\cdot(\boldsymbol{b}\times\boldsymbol{c}) = (\boldsymbol{a}\times\boldsymbol{b})\cdot\boldsymbol{c}$, yield

$$\int_{\partial\Omega}(\mathbb{A}\nabla u\cdot\boldsymbol{n} - \boldsymbol{F}\cdot\boldsymbol{n})v\,dS = \int_{\partial\Omega} gv\,dS - \alpha\left(\int_\Gamma u\boldsymbol{n}\,dS\right)\cdot\left(\int_\Gamma v\boldsymbol{n}\,dS\right) - \left(\mathbb{B}\int_\Gamma u\boldsymbol{r}\times\boldsymbol{n}\,dS\right)\cdot\left(\int_\Gamma v\boldsymbol{r}\times\boldsymbol{n}\,dS\right).$$

Combining together, we have

$$\mathscr{B}[u,v] = \int_\Omega fv\,dx + \int_\Omega \boldsymbol{F}\cdot\nabla v\,dx + \int_{\partial\Omega} gv\,dS. \tag{3.7}$$

where we set

$$\mathscr{B}[u,v] := \int_\Omega \mathbb{A}\nabla u\cdot\nabla v\,dx + \alpha\left(\int_\Gamma u\boldsymbol{n}\,dS\right)\cdot\left(\int_\Gamma v\boldsymbol{n}\,dS\right) + \mathbb{B}\left(\int_\Gamma u\boldsymbol{r}\times\boldsymbol{n}\,dS\right)\cdot\left(\int_\Gamma v\boldsymbol{r}\times\boldsymbol{n}\,dS\right). \tag{3.8}$$

We shall therefore say that a function $u\in H^1(\Omega)$ is a weak solution of the problem (3.2) – (3.4) if it satisfies the identity (3.7) for all $v\in H^1(\Omega)$.

By Lemma 2.1 and the assumption $\int_\Gamma \boldsymbol{r}\times\boldsymbol{n}\,dS = 0$, we have $\mathscr{B}[u,1]=0$ for any $u\in H^1(\Omega)$, and thus any weak solution of the problem (3.2) – (3.4) should satisfy the compatibility condition (3.6).

Next, we apply the Lax-Milgram theorem to show the existence of a weak solution. By the trace theorem, it is clear that $\mathscr{B}[\cdot,\cdot]$ is bounded; i.e., there is a constant C such that

$$|\mathscr{B}[u,v]| \le C\|u\|_{H^1(\Omega)}\|v\|_{H^1(\Omega)},\quad \forall u,\, v\in H^1(\Omega).$$

However, $\mathscr{B}[\cdot,\cdot]$ is not coercive on H^1. To remedy this, let us introduce a subspace $H^1_*(\Omega)$ of $H^1(\Omega)$ defined by

$$H^1_*(\Omega) := \{u\in H^1(\Omega) : \int_\Omega u = 0\}.$$

Clearly, $H^1_*(\Omega)$ is a closed subspace of $H^1(\Omega)$ and thus, $H^1_*(\Omega)$ itself is a Hilbert space. Let us recall that Poincaré's inequality:

$$\|u-(u)_\Omega\|_{L^2(\Omega)} \le C\|\nabla u\|_{L^2(\Omega)};\quad (u)_\Omega = \text{the average of } u \text{ over } \Omega.$$

When restricted to $H^1_*(\Omega)$, Poincaré's inequality and the assumption that $\alpha\ge 0$ and $\mathbb{B}\ge 0$ imply that $\mathscr{B}[\cdot,\cdot]$ is coercive on $H^1_*(\Omega)$; i.e., there is a constant $c>0$ such that

$$\mathscr{B}[u,u] \ge c\|u\|^2_{H^1(\Omega)},\quad \forall u\in H^1_*(\Omega). \tag{3.9}$$

As a matter of fact, for any $u\in H^1(\Omega)$, we have

$$\mathscr{B}[u,u] = \int_\Omega \mathbb{A}\nabla u\cdot\nabla u\,dx + \alpha\left|\int_\Gamma u\boldsymbol{n}\,dS\right|^2 + \mathbb{B}\left(\int_\Gamma u\boldsymbol{r}\times\boldsymbol{n}\,dS\right)\cdot\left(\int_\Gamma u\boldsymbol{r}\times\boldsymbol{n}\,dS\right) \ge \lambda\int_\Omega |\nabla u|^2\,dx, \tag{3.10}$$

and Poincaré's inequality yields (3.9). Also, the trace theorem verifies that the linear functional F on $H^1(\Omega)$ given by

$$F(v) := \int_\Omega fv\,dx + \int_\Omega \boldsymbol{F}\cdot\nabla v\,dx + \int_{\partial\Omega} gv\,dS \tag{3.11}$$

is bounded, and thus it is a bounded linear functional on $H^1_*(\Omega)$ as well.

Therefore, the Lax-Milgram theorem implies that there exists a unique $u \in H^1_*(\Omega)$ such that

$$\mathscr{B}[u,v] = F(v) = \int_\Omega fv\,dx + \int_\Omega \boldsymbol{F}\cdot\nabla v\,dx + \int_{\partial\Omega} gv\,dS, \quad \forall v \in H^1_*(\Omega).$$

We now show that u satisfies the identity (3.7) for any $v \in H^1(\Omega)$ so that u is indeed a weak solution of the problem (3.2) – (3.4). Note that any $v \in H^1(\Omega)$ can be written as $v = \tilde{v} + c$, where $\tilde{v} \in H^1_*(\Omega)$ and c is a constant. Since $\mathscr{B}[u,c] = 0$ by Lemma 2.1 and the assumption $\int_\Gamma \boldsymbol{r}\times\boldsymbol{n}\,dS = 0$, and $F(c) = 0$ by the compatibility condition (3.6), the identity (3.7) holds for u. Finally, we show that a weak solution u is unique modulo an additive constant. Thanks to linearity, it is enough to show that any $u \in H^1(\Omega)$ satisfying the identity

$$\mathscr{B}[u,v] = 0, \quad \forall v \in H^1(\Omega)$$

must be a constant. By taking $v = u$ in the above, we get by (3.10) that

$$0 = \mathscr{B}[u,u] \geq \lambda \int_\Omega |\nabla u|^2\,dx,$$

which obviously implies that u is a constant. ■

Remark 3.1. In fact, we can consider the case when $\Omega \subset \mathbb{R}^3$ is an (unbounded) exterior domain and $\Gamma' = \emptyset$. In this case, we also get a similar result except that we do not need to impose the compatibility condition. Here, we briefly describe the proof. Instead of working in $H^1(\Omega) = W^{1,2}(\Omega)$, we use a different function space $Y^{1,2}(\Omega)$, which is defined as the family of all weakly differentiable functions $u \in L^6(\Omega)$, whose weak derivatives are functions in $L^2(\Omega)$. The space $Y^{1,2}(\Omega)$ is endowed with the norm

$$\|u\|_{Y^{1,2}(\Omega)} := \|u\|_{L^6(\Omega)} + \|\nabla u\|_{L^2(\Omega)}.$$

It is known that if $\Omega = \mathbb{R}^3 \setminus \overline{D}$ and D is a bounded Lipschitz domain, then we have the following Sobolev inequality ([11]):

$$\|u\|_{L^6(\Omega)} \leq C\|\nabla u\|_{L^2(\Omega)}, \quad \forall u \in Y^{1,2}(\Omega). \tag{3.12}$$

Therefore, in this case, $Y^{1,2}(\Omega)$ becomes a Hilbert space under the inner product

$$\langle u,v\rangle_{Y^{1,2}(\Omega)} = \int_\Omega \nabla u\cdot\nabla v\,dx.$$

Also, we have the trace inequality

$$\|u\|_{L^2(\partial\Omega)} \leq C\|\nabla u\|_{L^2(\Omega)}, \quad \forall u \in Y^{1,2}(\Omega).$$

To see this, assume $\overline{D} \subset B(x_0,r)$ and fix $\eta \in C^\infty_c(B(x_0,2r))$ be such that $0 \leq \eta \leq 1$, $\eta = 1$ on $B(x_0,r)$, and $|\nabla\eta| \leq 2/r$; one may take $r = \operatorname{diam} D$. Denote $\Omega_r = \Omega \cap B(x_0,r)$. The usual trace inequality implies

$$\|\eta u\|_{L^2(\partial\Omega_{2r})} \leq C\|\eta u\|_{W^{1,2}(\Omega_{2r})}.$$

Note that $\|\eta u\|_{L^2(\partial\Omega_{2r})} = \|u\|_{L^2(\partial\Omega)}$ and $\|\eta u\|_{W^{1,2}(\Omega_{2r})} \leq C\|\nabla u\|_{L^2(\Omega)}$ by the Sobolev inequality (3.12) and Hölder's inequality. More precisely, we have

$$\int_{\Omega_{2r}} |\eta u|^2\,dx \leq Cr^2\left(\int_{\Omega_{2r}} |u|^6\,dx\right)^{\frac{1}{3}} \leq Cr^2\left(\int_\Omega |u|^6\,dx\right)^{\frac{1}{3}} \leq Cr^2\int_\Omega |\nabla u|^2\,dx$$

and similarly we get

$$\int_{\Omega_{2r}} |\nabla(\eta u)|^2\,dx \le 2\int_{\Omega_{2r}} \eta^2|\nabla u|^2\,dx + 2\int_{\Omega_{2r}} |\nabla\eta|^2|u|^2\,dx$$
$$\le 2\int_{\Omega_{2r}} |\nabla u|^2\,dx + C\int_{\Omega}|\nabla u|^2\,dx \le C\int_{\Omega}|\nabla u|^2\,dx.$$

Therefore, the bilinear form (3.8) is bounded and coercive on the Hilbert space $Y^{1,2}(\Omega)$. Also, if $\boldsymbol{F} \in L^2(\Omega)$, $f \in L^{6/5}(\Omega)$, and $g \in L^2(\partial\Omega)$, then the linear functional $F(\cdot)$ in (3.11) is bounded on $Y^{1,2}(\Omega)$, and thus Lax-Milgram theorem implies the existence of a weak solution.

Remark 3.2. We may also replace the boundary condition on Γ' to non-slip condition $\boldsymbol{U} = 0$.

3.2. **Regularity.** In this section, we study regularity of a weak solution $u \in H^1(\Omega)$ of the problem (3.2) – (3.4). As in the previous section, we assume that $\mathbb{A}$ satisfies the uniform ellipticity condition (3.5), $\alpha \ge 0$, $\mathbb{B} \ge 0$, and $\int_\Gamma \boldsymbol{r}\times\boldsymbol{n}\,dS = 0$.

Suppose f and g satisfy the compatibility condition (3.6) and let $u \in H^1(\Omega)$ be a weak solution of the problem (3.2) – (3.4). By Theorem 3.1, such a weak solution is unique up to an additive constant, and thus by Lemma 2.1 and the assumption $\int_\Gamma \boldsymbol{r}\times\boldsymbol{n}\,dS = 0$, we see that the (constant) vectors

$$\boldsymbol{a} := \int_\Gamma u\boldsymbol{n}\,dS \quad\text{and}\quad \boldsymbol{b} := \int_\Gamma u\boldsymbol{r}\times\boldsymbol{n}\,dS,$$

are uniquely determined (independent of an additive constant). Therefore, a weak solution $u \in H^1(\Omega)$ of the problem (3.2) – (3.4) is also a weak solution of

$$\begin{cases} -\nabla\cdot(\mathbb{A}\nabla u) = f - \nabla\cdot\boldsymbol{F} \ \text{ in } \ \Omega, \\ \mathbb{A}\nabla u\cdot\boldsymbol{n} = \boldsymbol{F}\cdot\boldsymbol{n} + g \ \text{ on } \ \Gamma', \\ \mathbb{A}\nabla u\cdot\boldsymbol{n} = \boldsymbol{F}\cdot\boldsymbol{n} + g - h \ \text{ on } \ \Gamma, \end{cases} \tag{3.13}$$

where we set

$$h := (\alpha\boldsymbol{a} + \mathbb{B}\boldsymbol{b}\times\boldsymbol{r})\cdot\boldsymbol{n} = \left[\alpha\int_{\partial\Omega} u\boldsymbol{n}\,dS + \left(\mathbb{B}\int_{\partial\Omega} u\boldsymbol{r}\times\boldsymbol{n}\,dS\right)\times\boldsymbol{r}\right]\cdot\boldsymbol{n}. \tag{3.14}$$

It is easy to check that

$$h \in L^\infty(\partial\Omega), \quad \int_{\partial\Omega} h\,dS = 0, \quad \text{and } h \text{ is as regular as } \boldsymbol{r}\times\boldsymbol{n}.$$

In particular, if $\boldsymbol{r} \in C^k(\Gamma;\mathbb{R}^d)$ and Γ is of class C^{k+1}, then $h \in C^k(\Gamma)$, etc. Therefore, we have the following results from the standard elliptic regularity theory and we omit the proofs because they are straightforwardly derived; see, e.g., [23, 15].

Theorem 3.2 (Interior H^k-regularity)**.** *Assume $\mathbb{A} \in C^{k+1}(\Omega)$, $f \in H^k(\Omega)$, and $\boldsymbol{F} \in H^{k+1}(\Omega)$, where $k \ge 0$ is an integer. If $u \in H^1(\Omega)$ is a weak solution of*

$$-\nabla\cdot(\mathbb{A}\nabla u) = f - \nabla\cdot\boldsymbol{F} \ \textit{ in } \ \Omega,$$

then $u \in H^{k+2}_{loc}(\Omega)$ and for $\Omega' \subset\subset \Omega$, we have the estimate

$$\|u\|_{H^{k+2}(\Omega')} \le C\left(\|f\|_{H^k(\Omega)} + \|\boldsymbol{F}\|_{H^{k+1}(\Omega)} + \|u\|_{L^2(\Omega)}\right).$$

where the constant C depends only on k, Ω, Ω', and $\mathbb{A}$.

Theorem 3.3 (Interior $C^{k+2,\alpha}$-regularity)**.** *Assume* $\mathbb{A} \in C^{k+1,\alpha}_{loc}(\Omega)$, $f \in C^{k,\alpha}_{loc}(\Omega)$, *and* $\boldsymbol{F} \in C^{k+1,\alpha}_{loc}(\Omega)$, *where* $k \geq 0$ *is an integer. If* $u \in H^1(\Omega)$ *is a weak solution of*

$$-\nabla \cdot (\mathbb{A}\nabla u) = f - \nabla \cdot \boldsymbol{F} \quad in \;\; \Omega,$$

then $u \in C^{k+2,\alpha}_{loc}(\Omega)$ *and for* $\Omega'' \subset\subset \Omega' \subset\subset \Omega$, *we have the estimate*

$$\|u\|_{C^{k+2,\alpha}(\Omega'')} \leq C \left(\|f\|_{C^{k,\alpha}(\Omega')} + \|\boldsymbol{F}\|_{C^{k+1,\alpha}(\Omega')} + \|u\|_{L^2(\Omega)} \right).$$

where the constant C *depends only on* k, Ω, Ω', *and* $\mathbb{A}$.

Theorem 3.4 (Global H^k-regularity)**.** *Assume* $\partial\Omega$ *is* C^{k+2}, $\mathbb{A} \in C^{k+1}(\overline{\Omega})$, $f \in H^k(\Omega)$, $\boldsymbol{F} \in H^{k+1}(\Omega)$, $g \in H^{k+\frac{1}{2}}(\partial\Omega)$, *and* $\boldsymbol{r} \in H^{k+\frac{1}{2}}(\Gamma)$, *where* $k \geq 0$ *is an integer. If* $u \in H^1(\Omega)$ *is a weak solution of the problem* (3.2) – (3.4), *then* $u \in H^{k+2}(\Omega)$. *In particular, if we fix* u *so that* $\int_\Omega u\,dx = 0$, *then we have the estimate*

$$\|u\|_{H^{k+2}(\Omega)} \leq C \left(\|f\|_{H^k(\Omega)} + \|\boldsymbol{F}\|_{H^{k+1}(\Omega)} + \|g\|_{H^{k+\frac{1}{2}}(\partial\Omega)} + \|\boldsymbol{r}\|_{H^{k+\frac{1}{2}}(\partial\Omega)} \right),$$

where the constant C *depends only on* Ω *and the coefficients* $\mathbb{A}$, α, $\mathbb{B}$.

Theorem 3.5 (Global $C^{k+2,\alpha}$-regularity)**.** *Let* $k \geq 0$ *be an integer and* $\alpha \in (0,1)$. *Assume* $\partial\Omega$ *is* $C^{k+2,\alpha}$, $\mathbb{A} \in C^{k+1,\alpha}(\Omega)$, $f \in C^{k,\alpha}(\Omega)$, $\boldsymbol{F} \in C^{k+1,\alpha}(\Omega)$, $g \in C^{k+1,\alpha}(\partial\Omega)$, *and* $\boldsymbol{r} \in C^{k+1,\alpha}(\Gamma)$. *If* $u \in H^1(\Omega)$ *be a weak solution of the problem* (3.2) – (3.4), *then* $u \in C^{k+2,\alpha}(\Omega)$. *In particular, if we fix* u *so that* $\int_\Omega u\,dx = 0$, *then we have the estimate*

$$\|u\|_{C^{k+2,\alpha}(\Omega)} \leq C \left(\|f\|_{C^{k,\alpha}(\Omega)} + \|\boldsymbol{F}\|_{C^{k+1,\alpha}(\Omega)} + \|g\|_{C^{k+1,\alpha}(\partial\Omega)} + \|\boldsymbol{r}\|_{C^{k+1,\alpha}(\partial\Omega)} \right),$$

where the constant C *depends only on* Ω *and the coefficients* $\mathbb{A}$, α, $\mathbb{B}$.

3.3. **Monolithic decomposition.** Now, we are ready to show the existence and uniqueness of the augmented Hodge decomposition with fluid-solid interaction mentioned in Section 2. As shown in the section, the decomposition is achieved monolithically as soon as we find the scalar field p.

Theorem 3.6 (Hodge decomposition with fluid-solid interaction)**.** *Let* $k \geq 0$ *be an integer and* $\alpha \in (0,1)$. *Assume* $\partial\Omega$ *is* C^{k+2} *(resp.,* $C^{k+2,\alpha}$*). Then, for any vector field* $\boldsymbol{U}^* \in H^{k+1}(\Omega)$ *(resp.,* $C^{k+1,\alpha}(\Omega)$*) and any linear and angular velocities* $\boldsymbol{v}^*, \boldsymbol{\omega}^* \in \mathbb{R}^d$, *the triple* $(\boldsymbol{U}^*, \boldsymbol{v}^*, \boldsymbol{\omega}^*)$ *are uniquely decomposed as*

$$\begin{cases} \rho \boldsymbol{U}^* = \rho \boldsymbol{U} + \nabla p \quad in \;\; \Omega \\ m\boldsymbol{v}^* = m\boldsymbol{v} - \displaystyle\int_\Gamma p\boldsymbol{n}\,dS \\ \mathbb{I}\boldsymbol{\omega}^* = \mathbb{I}\boldsymbol{\omega} - \displaystyle\int_\Gamma p\boldsymbol{J}\,dS \end{cases} \tag{3.15}$$

with a vector field $\boldsymbol{U} \in H^{k+1}(\Omega)$ *(resp.,* $C^{k+1,\alpha}(\Omega)$*),* $p \in H^{k+2}(\Omega)$ *(resp.,* $C^{k+2,\alpha}(\Omega)$*), and vectors* $\boldsymbol{v}, \boldsymbol{\omega} \in \mathbb{R}^d$ *that satisfy the incompressible condition and the non-penetration condition*

$$\begin{cases} \nabla \cdot \boldsymbol{U} = 0 \quad in \;\; \Omega, \\ \boldsymbol{U} \cdot \boldsymbol{n} = \boldsymbol{v} \cdot \boldsymbol{n} + \boldsymbol{\omega} \cdot \boldsymbol{J} \quad on \;\; \Gamma, \\ \boldsymbol{U} \cdot \boldsymbol{n} = 0 \quad on \;\; \Gamma'. \end{cases}$$

Proof. The decomposition (3.15) yields the following problem for the scalar field p:

$$\begin{cases} -\nabla\cdot\left(\dfrac{1}{\rho}\nabla p\right) = -\nabla\cdot\boldsymbol{U}^* \ \text{ in } \ \Omega, \\ \dfrac{1}{\rho}\dfrac{\partial p}{\partial n} + \boldsymbol{n}\cdot\dfrac{1}{m}\displaystyle\int_\Gamma p\boldsymbol{n}\,dS + \boldsymbol{J}\cdot\mathbb{I}^{-1}\int_\Gamma p\boldsymbol{J}\,dS = \boldsymbol{U}^*\cdot\boldsymbol{n} - \boldsymbol{v}^*\cdot\boldsymbol{n} - \boldsymbol{\omega}^*\cdot\boldsymbol{J} \ \text{ on } \ \Gamma, \\ \dfrac{1}{\rho}\dfrac{\partial p}{\partial n} = \boldsymbol{U}^*\cdot\boldsymbol{n} \ \text{ on } \ \Gamma'. \end{cases} \tag{3.16}$$

Set $\boldsymbol{F} = \boldsymbol{U}^*$, $f = 0$, and $g = -(\boldsymbol{v}^*\cdot\boldsymbol{n} + \boldsymbol{\omega}^*\cdot\boldsymbol{J})\chi_\Gamma$. Applying Lemma 2.1 for the compatibility condition and setting $\boldsymbol{r} := \boldsymbol{x} - \boldsymbol{c}$ so that $\boldsymbol{J} = \boldsymbol{r}\times\boldsymbol{n}$, Theorems 3.1 and 3.4 (resp., Theorem 3.5) imply that there exists a solution $p \in\in H^{k+2}(\Omega)$ (*resp.*, $C^{k+2,\alpha}(\Omega)$) of the problem (3.16). Then $\boldsymbol{U}, \boldsymbol{v}$, and $\boldsymbol{\omega}$ are defined as

$$\boldsymbol{U} = \boldsymbol{U}^* - \frac{1}{\rho}\nabla p, \quad \boldsymbol{v} = \boldsymbol{v}^* + \frac{1}{m}\int_\Gamma p\boldsymbol{n}\,dS, \quad \text{and} \quad \boldsymbol{\omega} = \boldsymbol{\omega}^* + \mathbb{I}^{-1}\left(\int_\Gamma p\boldsymbol{J}\,dS\right).$$

This shows the existence of a triple $(\boldsymbol{U}, \boldsymbol{v}, \boldsymbol{\omega})$ with $\boldsymbol{U} \in H^{k+1}(\Omega)$ (resp., $C^{k+1,\alpha}(\Omega)$) for the desired decomposition. Now, we show the uniqueness. To the end, by linearity it suffices to show that there exists only a trivial triple $(\boldsymbol{U}, \boldsymbol{v}, \boldsymbol{\omega}) = (0, 0, 0)$ satisfying

$$\rho\boldsymbol{U} = -\nabla p \ \text{ in } \ \Omega, \quad m\boldsymbol{v} = \int_\Gamma p\boldsymbol{n}\,dS, \quad \text{and} \quad \mathbb{I}\boldsymbol{\omega} = \int_\Gamma p\boldsymbol{J}\,dS \tag{3.17}$$

with the conditions $\nabla\cdot\boldsymbol{U} = 0$ in Ω, $\boldsymbol{U}\cdot\boldsymbol{n} = \boldsymbol{v}\cdot\boldsymbol{n} + \omega\cdot\boldsymbol{J}$ on Γ, and $\boldsymbol{U}\cdot\boldsymbol{n} = 0$ on Γ'. Taking into account all relations in terms of p, the scalar function p must satisfy

$$\begin{cases} -\nabla\cdot\left(\dfrac{1}{\rho}\nabla p\right) = 0 \ \text{ in } \ \Omega, \\ \dfrac{1}{\rho}\dfrac{\partial p}{\partial n} + \boldsymbol{n}\cdot\dfrac{1}{m}\displaystyle\int_\Gamma p\boldsymbol{n}\,dS + \boldsymbol{J}\cdot\mathbb{I}^{-1}\int_\Gamma p\boldsymbol{J}\,dS = 0 \ \text{ on } \ \Gamma, \\ \dfrac{1}{\rho}\dfrac{\partial p}{\partial n} = 0 \ \text{ on } \ \Gamma'. \end{cases}$$

In light of Theorem 3.1, we have that $\nabla p \equiv 0$, that is, p is constant. Therefore, by applying Lemma 2.1 to (3.17), we get that $\boldsymbol{U} = 0$, $\boldsymbol{v} = 0$, and $\boldsymbol{\omega} = 0$. We have thus shown that for an input $(\boldsymbol{U}^*, \boldsymbol{v}^*, \boldsymbol{\omega}^*)$ with $\boldsymbol{U}^* \in H^1(\Omega)$, there exists a unique $(\boldsymbol{U}, \boldsymbol{v}, \boldsymbol{\omega})$ satisfying the decomposition (3.15), which proves the theorem. ∎

4. Discretization by Heaviside function

4.1. **Heaviside function.** It is more convenient to express boundary conditions given on the interface $\Gamma = \partial\Omega$ in the entire domain $\mathbb{R}^d$. To do this, we consider the Heaviside function $H(x) = \chi_\Omega(x)$, which equal to 1 for $x \in \Omega$ and 0 elsewhere. Then $\nabla H = -\delta_\Gamma\boldsymbol{n}$, where δ_Γ is the Dirac delta function supported on Γ and $\boldsymbol{n}$ the outward normal vector at Γ. Using these notations, the boundary conditions (3.1) of p for the Helmholtz-Hodge decomposition (3.15) in fluid-solid interaction is represented as

$$-\nabla\cdot\left(\frac{H}{\rho}\nabla p\right)+\nabla H\cdot\frac{1}{m}\left(\int_{\mathbb{R}^d}p\nabla H\,dx\right)+(\boldsymbol{r}\times\nabla H)\cdot\mathbb{I}^{-1}\left(\int_{\mathbb{R}^d}p(\boldsymbol{r}\times\nabla H)\,dx\right) = -\nabla\cdot(H\boldsymbol{U}^*)+\boldsymbol{v}^*\cdot\nabla H+\boldsymbol{\omega}^*\cdot(\boldsymbol{r}\times\nabla H)\quad\text{in }\mathbb{R}^d. \tag{4.1}$$

with $\boldsymbol{r}=(\boldsymbol{x}-\boldsymbol{c})$. Based on the Heaviside formulation, we propose a numerical scheme to approximate p in the following subsection.

4.2. **Discretization based on Heaviside formulation.** In order to propose a numerical scheme for the problem, we introduce numerical settings. First, we consider the case $d=2$. Let $h\mathbb{Z}^2$ denote the uniform grid in $\mathbb{R}^2$ with step size h. For each grid node $(x_i,y_j)\in h\mathbb{Z}^2$, C_{ij} denotes the rectangular control volume centered at the node, and its four edges are denoted by $E_{i\pm\frac{1}{2},j}$ and $E_{i,j\pm\frac{1}{2}}$ as follows.

$$\begin{array}{rcccc} C_{ij} & := & [x_{i-\frac{1}{2}},x_{i+\frac{1}{2}}] & \times & [y_{j-\frac{1}{2}},y_{j+\frac{1}{2}}] \\ E_{i\pm\frac{1}{2},j} & := & x_{i\pm\frac{1}{2}} & \times & [y_{j-\frac{1}{2}},y_{j+\frac{1}{2}}] \\ E_{i,j\pm\frac{1}{2}} & := & [x_{i-\frac{1}{2}},x_{i+\frac{1}{2}}] & \times & y_{j\pm\frac{1}{2}} \end{array}$$

Based on the MAC configuration, we define the node set and the edge sets.

Definition 4.1. $\Omega^h:=\left\{(x_i,y_j)\in h\mathbb{Z}^2: C_{ij}\cap\Omega\neq\emptyset\right\}$ is the set of nodes whose control volumes intersect the domain. In the same way, edge sets are defined as

$$E^h_x:=\left\{(x_{i+\frac{1}{2}},y_j): E_{i+\frac{1}{2},j}\cap\Omega\neq\emptyset\right\},\quad E^h_y:=\left\{(x_i,y_{j+\frac{1}{2}}): E_{i,j+\frac{1}{2}}\cap\Omega\neq\emptyset\right\},$$

and $E^h:=E^h_x\cup E^h_y$.

Note that whenever $E_{i+\frac{1}{2},j}\cap\Omega\neq\emptyset$, $C_{ij}\cap\Omega\neq\emptyset$ and $C_{i+1,j}\cap\Omega\neq\emptyset$, since $E_{i+\frac{1}{2},j}\subset C_{ij}$ and $E_{i+\frac{1}{2},j}\subset C_{i+1,j}$.

In case when $d=3$, the settings and related definitions are almost the same as those for 2 dimensional case. Let $h\mathbb{Z}^3$ denote the uniform grid in $\mathbb{R}^3$ with step size h. For each grid node $(x_i,y_j,z_k)\in h\mathbb{Z}^3$, C_{ijk} denotes the hexahedron control volume centered at the node, and its six faces are denoted by $F_{i\pm\frac{1}{2},j,k}$ and $F_{i,j\pm\frac{1}{2},k}$ and $F_{i,j,k\pm\frac{1}{2}}$ as follows.

$$\begin{array}{rcccccc} C_{ijk} & := & [x_{i-\frac{1}{2}},x_{i+\frac{1}{2}}] & \times & [y_{j-\frac{1}{2}},y_{j+\frac{1}{2}}] & \times & [z_{k-\frac{1}{2}},z_{k+\frac{1}{2}}] \\ F_{i\pm\frac{1}{2},j,k} & := & x_{i\pm\frac{1}{2}} & \times & [y_{j-\frac{1}{2}},y_{j+\frac{1}{2}}] & \times & [z_{k-\frac{1}{2}},z_{k+\frac{1}{2}}] \\ F_{i,j\pm\frac{1}{2},k} & := & [x_{i-\frac{1}{2}},x_{i+\frac{1}{2}}] & \times & y_{j\pm\frac{1}{2}} & \times & [z_{k-\frac{1}{2}},z_{k+\frac{1}{2}}] \\ F_{i,j,k\pm\frac{1}{2}} & := & [x_{i-\frac{1}{2}},x_{i+\frac{1}{2}}] & \times & [y_{j-\frac{1}{2}},y_{j+\frac{1}{2}}] & \times & z_{k\pm\frac{1}{2}}. \end{array}$$

Similarly, we define the node set $\Omega^h=\left\{(x_i,y_j)\in h\mathbb{Z}^3: C_{ijk}\cap\Omega\neq\emptyset\right\}$ and the face sets F^h_x, F^h_y, F^h_z, and then $F^h=F^h_x\cup F^h_y\cup F^h_z$.

We split the node points into the inside points and the near-boundary points as

$$\Omega^h_\circ:=\{(x_i,y_j)\in\Omega^h: H_{i\pm\frac{1}{2},j}=H_{i,j\pm\frac{1}{2}}=1\}\quad\text{for }\ d=2,$$

$$\Omega^h_\circ:=\{(x_i,y_j,z_k)\in\Omega^h: H_{i\pm\frac{1}{2},j,k}=H_{i,j\pm\frac{1}{2},k}=H_{i,j,k\pm\frac{1}{2}}=1\}\quad\text{for }\ d=3,$$

and $\Omega^h_\Gamma:=\Omega^h\setminus\Omega^h_\circ$.

Since the arguments to the results given in this section are almost the same, we consider only the two dimensional case and the results can be extended easily to three dimension.

By the standard central finite differences, a discrete gradient and a discrete divergence operators are defined as follows.

Definition 4.2 (Discrete gradient and divergence operators)**.** By G_x, we denote the central finite differences in the x-direction:

$$(\mathrm{G}_x\, p)_{i+\frac{1}{2},j} = \frac{p_{i+1,j} - p_{i,j}}{h} \quad \text{and} \quad (\mathrm{G}_x\, u)_{i,j} = \frac{u_{i+\frac{1}{2},j} - u_{i-\frac{1}{2},j}}{h}.$$

Similarly, G_y denotes the central finite differences in the y-direction. The discrete gradient and divergence operators, denoted by G and D respectively, are defined as

$$\mathrm{G}[p_{i,j}] = \left([(\mathrm{G}_x\, p)_{i+\frac{1}{2},j}], [(\mathrm{G}_y\, p)_{i,j+\frac{1}{2}}]\right),$$
$$\mathrm{D}\left([u_{i+\frac{1}{2},j}], [v_{i,j+\frac{1}{2}}]\right) = [(\mathrm{G}_x\, u + \mathrm{G}_y\, v)_{ij}].$$

From the definitions of discrete gradient and divergence operators, we can see that one is the adjoint operator of the other. In other word, the two discrete operators satisfy the integration by parts.

Lemma 4.1 (Discrete integration by parts)**.** *Given a vector field and a scalar function*

$$\boldsymbol{U} = \left([u_{i+\frac{1}{2},j}], [v_{i,j+\frac{1}{2}}]\right) \quad \textit{and} \quad p = [p_{ij}]$$

with support E^h and Ω^h respectively, we have

$$\int (\mathrm{D}\,\boldsymbol{U}) p\, d\Omega^h := \sum_{i,j} (\mathrm{D}\,\boldsymbol{U})_{ij}\, p_{ij}\, h^2$$
$$= -\sum_{i,j} \left(u_{i+\frac{1}{2},j}\ \mathrm{G}_x\, p_{i+\frac{1}{2},j} + v_{i,j+\frac{1}{2}}\ \mathrm{G}_y\, p_{i,j+\frac{1}{2}}\right) h^2 =: -\int (\boldsymbol{U} \cdot \mathrm{G}\, p)\, d\Omega^h.$$

Proof. Using the definitions of discrete gradient and divergence operators, it is easy to show this lemma. ■

The Heaviside functions are defined on the edge set as follows.

Definition 4.3 (Heaviside function)**.** For each edge, the Heaviside function H is given as

$$H_{i+\frac{1}{2},j} = \frac{\mathrm{length}(E_{i+\frac{1}{2},j} \cap \Omega)}{\mathrm{length}(E_{i+\frac{1}{2},j})} \quad \text{and} \quad H_{i,j+\frac{1}{2}} = \frac{\mathrm{length}(E_{i,j+\frac{1}{2}} \cap \Omega)}{\mathrm{length}(E_{i,j+\frac{1}{2}})}.$$

Note that $H_{i+\frac{1}{2},j}$, $H_{i,j+\frac{1}{2}} \in [0,1]$ are equal to 1 if and only if the edge lies totally inside the domain, and 0 if and only if the edge lies completely outside.

For $d = 3$, the Heaviside functions are defined on F^h as follows.

$$H_{i+\frac{1}{2},j,k} = \frac{\mathrm{area}(F_{i+\frac{1}{2},j,k} \cap \Omega)}{\mathrm{area}(F_{i+\frac{1}{2},j,k})}, \quad H_{i,j+\frac{1}{2},k} = \frac{\mathrm{area}(F_{i,j+\frac{1}{2},k} \cap \Omega)}{\mathrm{area}(F_{i,j+\frac{1}{2},k})},$$
$$H_{i,j,k+\frac{1}{2}} = \frac{\mathrm{area}(F_{i,j,k+\frac{1}{2}} \cap \Omega)}{\mathrm{area}(F_{i,j,k+\frac{1}{2}})}.$$

Having defined discrete gradient and divergence operators and the discrete Heaviside function, we have the following lemma, which is analogous to Lemma 2.1.

Lemma 4.2. *The discrete Heaviside function* $H = [H_{i+\frac{1}{2},j}] \cup [H_{i,j+\frac{1}{2}}]$ *satisfies the relations*

$$\sum_{i,j} (\mathrm{G}\, H)_{ij} = 0 \quad \textit{and} \quad \sum_{i,j} ((x_i, y_j) - \boldsymbol{c}) \times (\mathrm{G}\, H)_{ij} = 0.$$

Proof. The proof is straightforward because every nonzero element of H appears twice with opposite sign in the summations. ■

Now, we are ready to formulate a discretization for Equation (3.1) based on the Heaviside representation (4.1). Using the settings and the definition of H defined as a scalar function on E^h, we derive a numerical scheme for p as

$$-\mathrm{D}\left(\frac{H}{\rho}\,\mathrm{G}\,p\right) + \mathrm{G}\,H \cdot \frac{1}{m}\left(\sum p\,\mathrm{G}\,H h^2\right) + \boldsymbol{J}^h \cdot \mathbb{I}^{-1}\left(\sum p \boldsymbol{J}^h h^2\right) = -\mathrm{D}(H\boldsymbol{U}^*) + \boldsymbol{v}^* \cdot \mathrm{G}\,H + \boldsymbol{\omega}^* \cdot \boldsymbol{J}^h \tag{4.2}$$

where $\boldsymbol{J}^h = (\boldsymbol{x} - \boldsymbol{c}) \times \mathrm{G}\,H$. More precisely, the terms on the left-hand side of Equation (4.2) read as

$$\begin{aligned}
\left(\mathrm{D}\left(\frac{H}{\rho}\,\mathrm{G}\,p\right)\right)_{ij} &= \frac{1}{h}\left(\frac{H_{i+\frac{1}{2},j}}{\rho_{i+\frac{1}{2},j}}\,\frac{p_{i+1,j} - p_{ij}}{h} - \frac{H_{i-\frac{1}{2},j}}{\rho_{i-\frac{1}{2},j}}\,\frac{p_{ij} - p_{i-1,j}}{h}\right) \\
&\quad + \frac{1}{h}\left(\frac{H_{i,j+\frac{1}{2}}}{\rho_{i,j+\frac{1}{2}}}\,\frac{p_{i,j+1} - p_{ij}}{h} - \frac{H_{i,j-\frac{1}{2}}}{\rho_{ij-\frac{1}{2}}}\,\frac{p_{ij} - p_{i,j-1}}{h}\right), \\
(\mathrm{G}\,H)_{ij} &= \left(\frac{H_{i+\frac{1}{2},j} - H_{i-\frac{1}{2},j}}{h},\ \frac{H_{i,j+\frac{1}{2}} - H_{i,j-\frac{1}{2}}}{h}\right), \\
(\boldsymbol{J}^h)_{ij} &= (\tilde{\boldsymbol{x}}_{ij} - \boldsymbol{c}) \times (\mathrm{G}\,H)_{ij}.
\end{aligned}$$

where $\tilde{\boldsymbol{x}}_{ij}$ is given as

$$\tilde{\boldsymbol{x}}_{ij} = \begin{cases} \frac{1}{2}(\boldsymbol{x} + \boldsymbol{y}) & \text{if} \quad \partial C_{ij} \cap \partial\Omega = \{\boldsymbol{x}, \boldsymbol{y}\}, \\ 0 & \text{if} \quad \partial C_{ij} \cap \partial\Omega = \emptyset. \end{cases}$$

4.3. **Stability.** Let $L^h : \mathbb{R}^{|\Omega^h|} \to \mathbb{R}^{|\Omega^h|}$ be a linear operator associated with the left-hand side of (4.2). Then the linear system (4.2) reads as: Given a triple $(\boldsymbol{U}^*, \boldsymbol{v}^*, \boldsymbol{\omega}^*)$, find a scalar function $p : \Omega^h \to \mathbb{R}$ satisfying

$$L^h p = -\mathrm{D}(H\boldsymbol{U}^*) + \boldsymbol{v}^* \cdot \mathrm{G}\,H + \boldsymbol{\omega}^* \cdot \boldsymbol{J}^h. \tag{4.3}$$

In order to verify the existence of p, we first estimate some properties of L^h.

Lemma 4.3. *The linear operator* L^h *is symmetric and positive semi-definite on* $\mathbb{R}^{|\Omega^h|}$ *and* $\ker(L^h) = \mathrm{Span}\{1_{\Omega^h}\}$ *where* 1_{Ω^h} *is the function for which* $1_{\Omega^h} \equiv 1$ *on* Ω^h.

Proof. Let $p^{(1)}, p^{(2)} \in \mathbb{R}^{|\Omega^h|}$ be arbitrarily given. The discrete integration by parts shown in Lemma 4.1 implies

$$
\begin{aligned}
&\langle L^h p^{(1)}, p^{(2)}\rangle \\
&= -\sum_{i,j} p_{ij}^{(2)} \left(\mathrm{D}\left(\frac{H}{\rho}\,\mathrm{G}\,p^{(1)}\right)\right)_{ij} + \sum_{i,j} p_{ij}^{(2)}\,(\mathrm{G}\,H)_{ij}\cdot\frac{1}{m}\left(\sum_{k,l} p_{kl}^{(1)}(\mathrm{G}\,H)_{kl}\,h^2\right) \\
&\qquad + \sum_{i,j} p_{ij}^{(2)}(\boldsymbol{J}^h)_{ij}\cdot\mathbb{I}^{-1}\left(\sum_{k,l} p_{kl}^{(1)}(\boldsymbol{J}^h)_{kl}\,h^2\right) \\
&= \sum_{i,j}\frac{H_{i+\frac12,j}}{\rho_{i+\frac12,j}}(\mathrm{G}_x\,p^{(2)})_{i+\frac12,j}(\mathrm{G}_x\,p^{(1)})_{i+\frac12,j} + \sum_{i,j}\frac{H_{i,j+\frac12}}{\rho_{i,j+\frac12}}(\mathrm{G}_y\,p^{(2)})_{i,j+\frac12}(\mathrm{G}_y\,p^{(1)})_{i,j+\frac12} \\
&\qquad + \frac{h^2}{m}\left(\sum_{i,j} p_{ij}^{(2)}(\mathrm{G}\,H)_{ij}\right)\cdot\left(\sum_{k,l} p_{kl}^{(1)}(\mathrm{G}\,H)_{kl}\right) \\
&\qquad + h^2\left(\sum_{i,j} p_{ij}^{(2)}(\boldsymbol{J}^h)_{ij}\right)\cdot\mathbb{I}^{-1}\left(\sum_{k,l} p_{kl}^{(1)}(\boldsymbol{J}^h)_{kl}\right) \\
&= \langle p^{(1)}, L^h p^{(2)}\rangle
\end{aligned}
$$

and the symmetry of $\mathbb{I}^{-1}$ shows that L^h is symmetric. In particular, if $p^{(1)} = p^{(2)}$, we have

$$
\begin{aligned}
\langle L^h p^{(1)}, p^{(1)}\rangle &= \sum_{i,j}\frac{H_{i+\frac12,j}}{\rho_{i+\frac12,j}}(\mathrm{G}_x\,p^{(1)})^2_{i+\frac12,j} + \sum_{i,j}\frac{H_{i,j+\frac12}}{\rho_{i,j+\frac12}}(\mathrm{G}_y\,p^{(1)})^2_{i,j+\frac12} \\
&\qquad + \frac{h^2}{m}\left|\sum_{i,j} p_{ij}^{(1)}(\mathrm{G}\,H)_{ij}\right|^2 + h^2\left(\sum_{i,j} p_{ij}^{(1)}(\boldsymbol{J}^h)_{ij}\right)\cdot\mathbb{I}^{-1}\left(\sum_{k,l} p_{kl}^{(1)}(\boldsymbol{J}^h)_{k\ell}\right),
\end{aligned}
$$

which implies that $\langle L^h p, p\rangle \geq 0$ for all $p \in \mathbb{R}^{|\Omega^h|}$ because the inertia matrix $\mathbb{I}$ is positive-definite; hence, L^h is positive semi-definite. Let $p \in \ker(L^h)$. Then we have $\langle L^h p, p\rangle = 0$, which implies

$$(\mathrm{G}_x\,p)_{i+\frac12,j} = (\mathrm{G}_x\,p)_{i+\frac12,j} = 0, \quad \forall (x_i, y_j) \in \Omega^h.$$

This implies that $p_{ij} = p_{i+1,j} = p_{i,j+1}$ for all $(x_i, y_j) \in \Omega^h$, so that p is constant. Conversely, if p is a constant vector, then Lemma 4.2 shows that $L^h p = 0$. This completes the proof. ∎

The following theorem shows the existence and uniqueness condition of the solution for the linear system $L^h p = f$.

Theorem 4.1. *The linear equation $L^h p = f$ is solvable if and only if $\sum_{i,j} f_{ij} = 0$. Furthermore, there exists a unique solution $p \in \{1_{\Omega^h}\}^\perp$.*

Proof. Since L^h is symmetric, Lemma 4.3 implies that the range of L^h, denoted by $R(L^h)$, is the orthogonal complement of $\mathrm{Span}\{1_{\Omega^h}\}$; that is, $R(L^h) = \{1_{\Omega^h}\}^\perp$. Also, the lemma yields that L^h is symmetric positive definite on $R(L^h)$ so that for $f \in \{1_{\Omega^h}\}^\perp$, the equation $L^h p = f$ has a unique solution $p \in \{1_{\Omega^h}\}^\perp$. ∎

Theorem 4.1 may be regarded as an analogy of the compatibility condition shown in Theorem 3.1 in the following sense. Given a triple $(\boldsymbol{U}^*, \boldsymbol{v}^*, \boldsymbol{\omega}^*)$, consider the problem of finding a scalar function $p : \Omega^h \to \mathbb{R}$ satisfying

$$L^h p = -\,\mathrm{D}\,(H\boldsymbol{U}^*) + \boldsymbol{v}^* \cdot \mathrm{G}\,H + \boldsymbol{\omega}^* \cdot \boldsymbol{J}^h \quad \text{in} \quad \Omega^h. \tag{4.4}$$

Theorem 4.1 shows that the linear system (4.4) is solvable if and only if

$$-\,\mathrm{D}(H\boldsymbol{U}^*) + \boldsymbol{v}^* \cdot \mathrm{G}\,H + \boldsymbol{\omega}^* \cdot \boldsymbol{J}^h \in \{1_{\Omega^h}\}^\perp,$$

that is,

$$\sum_{(x_i,y_j)\in\Omega^h} \Big(-\,\mathrm{D}(H\boldsymbol{U}^*) + \boldsymbol{v}^* \cdot \mathrm{G}\,H + \boldsymbol{\omega}^* \cdot \boldsymbol{J}^h\Big)_{ij} = 0, \tag{4.5}$$

Precisely, the problem (4.4) reads as

$$-\,\mathrm{D}\left(\frac{1}{\rho}\,\mathrm{G}\,p\right) = -\,\mathrm{D}\,\boldsymbol{U}^* \quad \text{in} \quad \Omega^h_\circ$$

and

$$\begin{aligned} -\,\mathrm{D}\left(\frac{H}{\rho}\,\mathrm{G}\,p\right) + \mathrm{G}\,H \cdot \frac{1}{m}\left(\sum p\,\mathrm{G}\,H\,h^2\right) + \boldsymbol{J}^h \cdot \mathbb{I}^{-1}\left(\sum p\boldsymbol{J}^h\,h^2\right)& \\ = -\,\mathrm{D}(H\boldsymbol{U}^*) + \boldsymbol{v}^* \cdot \mathrm{G}\,H + \boldsymbol{\omega}^* \cdot \boldsymbol{J}^h \quad \text{in} \quad \Omega^h_\Gamma.& \end{aligned}$$

Also, splitting the summation on the left-hand side of (4.5), we have

$$-\sum_{(x_i,y_j)\in\Omega^h_o} (\mathrm{D}\,\boldsymbol{U}^*)_{ij} + \sum_{(x_i,y_j)\in\Omega^h_\Gamma} \Big(-\,\mathrm{D}(H\boldsymbol{U}^*) + \boldsymbol{v}^* \cdot \mathrm{G}\,H + \boldsymbol{\omega}^* \cdot \boldsymbol{J}^h\Big)_{ij} = 0.$$

This is a discrete version of compatibility condition.

Once p is solved, the triple $(\boldsymbol{U}^*, \boldsymbol{v}^*, \boldsymbol{\omega}^*)$ is decomposed as

$$(\boldsymbol{U}^*, \boldsymbol{v}^*, \boldsymbol{\omega}^*) = (\boldsymbol{U}, \boldsymbol{v}, \boldsymbol{\omega}) + \left(\frac{1}{\rho}\,\mathrm{G}\,p,\ \frac{1}{m}\sum_{k,l}(p\,\mathrm{G}\,H)_{kl}\,h^2,\ \mathbb{I}^{-1}\sum_{k,l}(p\boldsymbol{J}^h)_{kl}\,h^2\right).$$

Now, we are to show that the decomposition is unique with p satisfying (4.4) and orthogonal with respect to the inner product $\langle\cdot,\cdot\rangle_{E_h}$ defined by

$$\Big\langle(\boldsymbol{U}^h_1, \boldsymbol{v}^h_1, \boldsymbol{\omega}^h_1), (\boldsymbol{U}^h_2, \boldsymbol{v}^h_2, \boldsymbol{\omega}^h_2)\Big\rangle_{E_h} := \int \frac{1}{2}\rho H \boldsymbol{U}^h_1 \cdot \boldsymbol{U}^h_2\, d\Omega^h + \frac{1}{2} m \boldsymbol{v}^h_1 \cdot \boldsymbol{v}^h_2 + \frac{1}{2}\boldsymbol{\omega}^h_1 \cdot \mathbb{I}\boldsymbol{\omega}^h_2. \tag{4.6}$$

Theorem 4.2. *Given a triple $(\boldsymbol{U}^*, \boldsymbol{v}^*, \boldsymbol{\omega}^*)$, there exists a unique $p \in \{1_{\Omega^h}\}^\perp$ satisfying*

$$L^h p = -\,\mathrm{D}(H\boldsymbol{U}^*) + \boldsymbol{v}^* \cdot \mathrm{G}\,H + \boldsymbol{\omega}^* \cdot \boldsymbol{J}^h \quad \textit{in} \quad \Omega^h. \tag{4.7}$$

Therefore, the triple $(\boldsymbol{U}^*, \boldsymbol{v}^*, \boldsymbol{\omega}^*)$ is uniquely decomposed as

$$(\boldsymbol{U}^*, \boldsymbol{v}^*, \boldsymbol{\omega}^*) = (\boldsymbol{U}, \boldsymbol{v}, \boldsymbol{\omega}) + \left(\frac{1}{\rho}\,\mathrm{G}\,p,\ \frac{1}{m}\sum_{k,l}(p\,\mathrm{G}\,H)_{kl}\,h^2,\ \mathbb{I}^{-1}\sum_{k,l}(p\boldsymbol{J}^h)_{kl}h^2\right) \tag{4.8}$$

with p satisfying (4.7)*. Furthermore, the decomposition is orthogonal with respect to the inner product* (4.6)*.*

Proof. Lemmas 4.1 and 4.2 show the solvability condition

$$\sum_{(x_i,y_j)\in\Omega^h}\Big(-\mathrm{D}(H\boldsymbol{U}^*)+\boldsymbol{v}^*\cdot\mathrm{G}\,H+\boldsymbol{\omega}^*\cdot\boldsymbol{J}^h\Big)_{ij}$$
$$=\int(H\boldsymbol{U}^*\cdot\mathrm{G}\,1_{\Omega^h})\,d\Omega^h+\boldsymbol{v}^*\cdot\int(\mathrm{G}\,H)\,d\Omega^h+\boldsymbol{\omega}^*\cdot\int\boldsymbol{J}^h\,d\Omega^h=0.$$

Then, Theorem 4.1 verifies the existence and uniqueness of p in $\{1_{\Omega^h}\}^{\perp}$. With such p, we decompose $(\boldsymbol{U}^*,\boldsymbol{v}^*,\boldsymbol{w}^*)$ as

$$(\boldsymbol{U}^*,\boldsymbol{v}^*,\boldsymbol{\omega}^*)=(\boldsymbol{U},\boldsymbol{v},\boldsymbol{\omega})+\left(\frac{1}{\rho}\mathrm{G}\,p,\ \frac{1}{m}\sum_{k,l}(p\,\mathrm{G}\,H)_{kl}\,h^2,\ \mathbb{I}^{-1}\sum_{k,l}(p\boldsymbol{J}^h)_{kl}\,h^2\right).$$

Applying the decomposition to (4.7) shows

$$-\mathrm{D}(H\boldsymbol{U})+\mathrm{G}\,H\cdot\boldsymbol{v}+\boldsymbol{J}^h\cdot\boldsymbol{\omega}=0\quad\text{in}\quad\Omega^h.$$

Using the identity above and Lemma 4.1, we have

$$\begin{aligned}&\left\langle(\boldsymbol{U},\boldsymbol{v},\boldsymbol{\omega}),\left(\frac{1}{\rho}\mathrm{G}\,p,\ \frac{1}{m}\sum_{k,l}(p\,\mathrm{G}\,H)_{kl}\,h^2,\ \mathbb{I}^{-1}\sum_{k,l}(p\boldsymbol{J}^h)_{kl}\,h^2\right)\right\rangle_{E_h}\\&=\int\frac{1}{2}\rho H\boldsymbol{U}\cdot\left(\frac{1}{\rho}\mathrm{G}\,p\right)d\Omega^h+\frac{1}{2}m\boldsymbol{v}\cdot\left(\frac{1}{m}\int p\,\mathrm{G}\,H\,d\Omega^h\right)+\frac{1}{2}\boldsymbol{\omega}\cdot\left(\int p\boldsymbol{J}^h\,d\Omega^h\right)\\&=\frac{1}{2}\int p(-\mathrm{D}(H\boldsymbol{U})+\boldsymbol{v}\cdot\mathrm{G}\,H+\boldsymbol{\omega}\cdot\boldsymbol{J}^h)\,d\Omega^h=0.\end{aligned}$$

This shows the orthogonality of the decomposition with respect to the inner product (4.6). The uniqueness of the decomposition is verified from Theorem 4.1, which completes the proof. ■

The following theorem demonstrates that the discrete projection $(\boldsymbol{U},\boldsymbol{v},\boldsymbol{\omega})$ of $(\boldsymbol{U}^*,\boldsymbol{v}^*,\boldsymbol{\omega}^*)$ is stable in the sense that it does not increase the kinetic energy:

Theorem 4.3. *Assume the kinetic energy of a triple $(\boldsymbol{U}^*,\boldsymbol{v}^*,\boldsymbol{\omega}^*)$ with $\boldsymbol{U}^*=(U_x^*,U_y^*)$ is discretized as*

$$\begin{aligned}E_h&=\frac{1}{2}\int(\rho H\boldsymbol{U}^*\cdot\boldsymbol{U}^*)\,d\Omega^h+\frac{1}{2}m\boldsymbol{v}^*\cdot\boldsymbol{v}^*+\frac{1}{2}\boldsymbol{\omega}^*\cdot\mathbb{I}\boldsymbol{\omega}^*\\&=\frac{1}{2}\sum_{i,j}\Big((\rho H(U_x^*)^2)_{i+\frac{1}{2},j}+(\rho H(U_y^*)^2)_{i,j+\frac{1}{2}}\Big)\,h^2+\frac{1}{2}m|\boldsymbol{v}^*|^2+\frac{1}{2}\boldsymbol{\omega}^*\mathbb{I}\boldsymbol{\omega}^*.\end{aligned}$$

If the system $(\boldsymbol{U}^*,\boldsymbol{v}^*,\boldsymbol{\omega}^*)$ is projected into $(\boldsymbol{U},\boldsymbol{v},\boldsymbol{\omega})$ given by

$$(\boldsymbol{U},\boldsymbol{v},\boldsymbol{\omega})=(\boldsymbol{U}^*,\boldsymbol{v}^*,\boldsymbol{\omega}^*)-\left(\frac{1}{\rho}\mathrm{G}\,p,\ \frac{1}{m}\sum_{k,l}(p\,\mathrm{G}\,H)_{kl}\,h^2,\ \mathbb{I}^{-1}\sum_{k,l}(p\boldsymbol{J}^h)_{kl}\,h^2\right)$$

where $p\in\{1_{\Omega^h}\}^{\perp}$ is the solution to the problem (4.7). Then, the discrete projection is stable in the sense $E_h(\boldsymbol{U}^*,\boldsymbol{v}^*,\boldsymbol{\omega}^*)\geq E_h(\boldsymbol{U},\boldsymbol{v},\boldsymbol{\omega})$.

Proof. From the orthogonality shown in Theorem 4.2, we conclude

$$E_h(\boldsymbol{U}^*, \boldsymbol{v}^*, \boldsymbol{\omega}^*) = \langle(\boldsymbol{U}^*, \boldsymbol{v}^*, \boldsymbol{\omega}^*), (\boldsymbol{U}^*, \boldsymbol{v}^*, \boldsymbol{\omega}^*)\rangle_{E_h} \geq \langle(\boldsymbol{U}, \boldsymbol{v}, \boldsymbol{\omega}), (\boldsymbol{U}, \boldsymbol{v}, \boldsymbol{\omega})\rangle_{E_h} = E_h(\boldsymbol{U}, \boldsymbol{v}, \boldsymbol{\omega})$$

and this shows the decrease of the kinetic energy. ∎

5. Convergence analysis

In this section, we estimate the consistency and convergence of the numerical scheme. In the previous sections, we have decomposed a given triple $(\boldsymbol{U}^*, \boldsymbol{v}^*, \boldsymbol{\omega}^*)$ using the Heaviside function $H = \chi_\Omega$ as

$$(\boldsymbol{U}^*, \boldsymbol{v}^*, \boldsymbol{\omega}^*) = (\boldsymbol{U}, \boldsymbol{v}, \boldsymbol{\omega}) + \left(\frac{1}{\rho}\nabla p,\ -\frac{1}{m}\int_\Gamma p\boldsymbol{n}\, dS,\ -\mathbb{I}^{-1}\int_\Gamma p\boldsymbol{J}\, dS\right) \tag{5.1}$$

by solving the equation

$$\mathcal{L}(\boldsymbol{U}, \boldsymbol{v}, \boldsymbol{\omega}) := -\nabla\cdot(H\boldsymbol{U}) + \nabla H\cdot \boldsymbol{v} + (\boldsymbol{x}-\boldsymbol{c})\times\nabla H\cdot\boldsymbol{\omega} = 0 \quad \text{in} \quad \mathbb{R}^d \tag{5.2}$$

with the conditions

$$\begin{cases} \nabla\cdot\boldsymbol{U} = 0 & \text{in} \quad \Omega \\ \boldsymbol{U}\cdot\boldsymbol{n} = \boldsymbol{v}\cdot\boldsymbol{n} + \boldsymbol{\omega}\cdot\boldsymbol{J} & \text{on} \quad \Gamma = \partial\Omega. \end{cases}$$

Then the numerical approximation $(\boldsymbol{U}^h, \boldsymbol{v}^h, \boldsymbol{\omega}^h)$ to $(\boldsymbol{U}, \boldsymbol{v}, \boldsymbol{\omega})$ has been obtained by solving the linear system

$$\mathcal{L}^h(\boldsymbol{U}^h, \boldsymbol{v}^h, \boldsymbol{\omega}^h) := -\,\mathrm{D}(H\boldsymbol{U}^h) + \mathrm{G}\,H\cdot\boldsymbol{v}^h + \boldsymbol{J}^h\cdot\boldsymbol{\omega}^h = 0 \quad \text{in} \quad \Omega^h \tag{5.3}$$

using the decomposition

$$(\boldsymbol{U}^*, \boldsymbol{v}^*, \boldsymbol{\omega}^*) = (\boldsymbol{U}^h, \boldsymbol{v}^h, \boldsymbol{\omega}^h) + \left(\frac{1}{\rho}\,\mathrm{G}\,p^h,\ \frac{1}{m}\sum_{i,j,k}(p^h\,\mathrm{G}\,H)_{ijk}h^3,\ \mathbb{I}^{-1}\sum_{i,j,k}(p^h\boldsymbol{J}^h)_{ijk}h^3\right) \tag{5.4}$$

where $p^h \in \{1_{\Omega^h}\}^\perp$.

By $(\boldsymbol{U}, \boldsymbol{v}, \boldsymbol{\omega})$ and $(\boldsymbol{U}^h, \boldsymbol{v}^h, \boldsymbol{\omega}^h)$, throughout this section, we denote the continuous and numerical solutions, respectively. In the setting, let $(\boldsymbol{U}_e, \boldsymbol{v}_e, \boldsymbol{\omega}_e) := (\boldsymbol{U}-\boldsymbol{U}^h, \boldsymbol{v}-\boldsymbol{v}^h, \boldsymbol{\omega}-\boldsymbol{\omega}^h)$ denote the convergence error. The consistency error for numerical scheme is defined as

$$c^h := \mathcal{L}^h(\boldsymbol{U}, \boldsymbol{v}, \boldsymbol{\omega}) - \mathcal{L}^h(\boldsymbol{U}^h, \boldsymbol{v}^h, \boldsymbol{\omega}^h).$$

In order to estimate the consistency, we need the following lemma.

Lemma 5.1. *We have the followings.*

(i) *For $d = 2$, we have on $C_{ij}\cap\partial\Omega$*

$$\int_{C_{ij}\cap\Gamma} \boldsymbol{n}\, dS = -(\mathrm{G}\,H)_{ij}h^2 \quad \textit{and} \quad \int_{C_{ij}\cap\Gamma} \boldsymbol{J}\, dS = -\left(\boldsymbol{J}^h\right)_{ij}h^2$$

where $(\boldsymbol{J}^h)_{ij} = (0,0)$ if $\partial C_{ij}\cap\Gamma = \emptyset$ and $(\boldsymbol{J}^h)_{ij} = (\frac{\boldsymbol{x}_1+\boldsymbol{x}_2}{2}-\boldsymbol{c})\times(\mathrm{G}\,H)_{ij}$ if $\partial C_{ij}\cap\Gamma = \{\boldsymbol{x}_1, \boldsymbol{x}_2\}$.

(ii) *For $d=3$, we have on $C_{ijk}\cap\partial\Omega$*

$$\int\limits_{C_{ijk}\cap\Gamma} \boldsymbol{n}\,dS = -(\mathrm{G}\,H)_{ijk}h^3 \quad \textit{and} \quad \int\limits_{C_{ijk}\cap\Gamma} \boldsymbol{J}\,dS = -(\boldsymbol{J}^h)_{ijk}h^3 + h^3\boldsymbol{\varepsilon}_{ijk}$$

where $(\boldsymbol{J}^h)_{ijk}=(0,0,0)$ if $\partial C_{ijk}\cap\Gamma=\emptyset$ and $(\boldsymbol{J}^h)_{ijk}=(\boldsymbol{x}_{ijk}-\boldsymbol{c})\times(\mathrm{G}\,H)_{ijk}$ if $\partial C_{ijk}\cap\Gamma\neq\emptyset$, and

$$h^3\boldsymbol{\varepsilon}_{ijk} = \int\limits_{C_{ijk}\cap\Gamma} (\boldsymbol{x}-\boldsymbol{x}_{ijk})\times\boldsymbol{n}\,dS. \tag{5.5}$$

(iii) *For $d=2,3$ we have on $\Gamma=\partial\Omega$*

$$\left|\int_\Gamma p\boldsymbol{n}\,dS + \sum_{\boldsymbol{x}_h\in\Omega_\Gamma^h}(pGH)_{\boldsymbol{x}_h}h^d\right| \le \frac{\sqrt{d}\,|\Gamma|\,\|\nabla p\|_{L^\infty}}{2}\,h, \tag{5.6}$$

$$\left|\int_\Gamma p\boldsymbol{J}\,dS + \sum_{\boldsymbol{x}_h\in\Omega_\Gamma^h}(p\boldsymbol{J}^h)_{\boldsymbol{x}_h}h^d\right| \le \frac{\sqrt{d}\,|\Gamma|\,\big((\operatorname{diam}\Gamma)\,\|\nabla p\|_{L^\infty}+\delta_{d,3}\|p\|_{L^\infty}\big)}{2}\,h, \tag{5.7}$$

where δ is the Kronecker delta symbol.

Proof. (i) Let $\boldsymbol{n}$ be the outward unit normal vector of $\partial(C_{ij}\cap\Omega)$. Then the same argument used for the proof of Lemma 2.1 shows

$$\int\limits_{\partial(C_{ij}\cap\Omega)} \boldsymbol{n}\,dS = 0 \quad \text{and} \quad \int\limits_{\partial(C_{ij}\cap\Omega)} \boldsymbol{J}\,dS = 0.$$

These imply

$$\int\limits_{C_{ij}\cap\Gamma} \boldsymbol{n}\,dS = -\int\limits_{\partial C_{ij}\cap\Omega} \boldsymbol{n}\,dS = -(\mathrm{G}\,H)_{ij}\,h^2$$

and

$$\int\limits_{C_{ij}\cap\Gamma} \boldsymbol{J}\,dS = -\int\limits_{\partial C_{ij}\cap\Omega} \boldsymbol{J}\,dS = -(\boldsymbol{J}^h)_{ij}\,h^2,$$

where $(\boldsymbol{J}^h)_{ij}=(0,0)$ if $\partial C_{ij}\cap\Gamma=\emptyset$ and $(\boldsymbol{J}^h)_{ij}=(\frac{\boldsymbol{x}_1+\boldsymbol{x}_2}{2}-\boldsymbol{c})\times(\mathrm{G}\,H)_{ij}$ if $\partial C_{ij}\cap\Gamma=\{\boldsymbol{x}_1,\boldsymbol{x}_2\}$.

(ii) Using the similar argument used for the proof of (i), one can show

$$\int\limits_{C_{ijk}\cap\Gamma} \boldsymbol{n}\,dS = -(\mathrm{G}\,H)_{ijk}\,h^3 \quad \text{and} \quad \int\limits_{C_{ijk}\cap\Gamma} \boldsymbol{J}\,dS = -(\boldsymbol{J}^h)_{ijk}\,h^3 + h^3\boldsymbol{\varepsilon}_{ijk}$$

with $\boldsymbol{\varepsilon}_{ijk}$ given in (5.5).

(iii) Using (i) and (ii), we have

$$\begin{aligned}\left|\int_\Gamma p\boldsymbol{n}\,dS + \sum_{\boldsymbol{x}_h\in\Omega_\Gamma^h}(pGH)_{\boldsymbol{x}_h}h^d\right| &\le \sum_{\boldsymbol{x}_h\in\Omega_\Gamma^h}\int_{\Gamma\cap C_{\boldsymbol{x}_h}}|p(\boldsymbol{x})-p(\boldsymbol{x}_h)|\,dS\\ &\le \sum_{\boldsymbol{x}_h\in\Omega_\Gamma^h}\frac{\sqrt{d}\,\|\nabla p\|_{L^\infty}}{2}\,h\int_{\Gamma\cap C_{\boldsymbol{x}_h}}dS\\ &= \frac{\sqrt{d}\,|\Gamma|\,\|\nabla p\|_{L^\infty}}{2}\,h.\end{aligned}$$

Here, we used that for $\boldsymbol{x}_h\in\Omega_\Gamma^h$ and $\boldsymbol{x}\in\Gamma\cap C_{\boldsymbol{x}_h}$, we have

$$|p(\boldsymbol{x})-p(\boldsymbol{x}_h)|\le|\boldsymbol{x}-\boldsymbol{x}_h|\,\|\nabla p\|_{L^\infty}\le\frac{\sqrt{d}\,\|\nabla p\|_{L^\infty}}{2}\,h.$$

So, we have shown the inequality (5.6). To show (5.7), we apply (i) and (ii) to obtain

$$\begin{aligned}\int_\Gamma p\boldsymbol{J}\,dS + \sum_{\boldsymbol{x}_h\in\Omega_\Gamma^h}\left(p\boldsymbol{J}^h\right)_{\boldsymbol{x}_h}h^d &= \sum_{\boldsymbol{x}_h\in\Omega_\Gamma^h}\int_{\Gamma\cap C_{\boldsymbol{x}_h}}(p(\boldsymbol{x})-p(\boldsymbol{x}_h))\boldsymbol{J}dS\\ &\quad+\delta_{d,3}\sum_{\boldsymbol{x}_h\in\Omega_\Gamma^h}\int_{\Gamma\cap C_{\boldsymbol{x}_h}}p(\boldsymbol{x}_h)(\boldsymbol{x}-\boldsymbol{x}_h)\times\boldsymbol{n}\,dS.\end{aligned}$$

Applying the similar argument to obtain (5.6) leads to the inequality (5.7). ■

Theorem 5.1 (Consistency error)**.** *Let $(\boldsymbol{U},\boldsymbol{v},\boldsymbol{\omega})$ be the continuous solution to* (5.1) - (5.2) *and $(\boldsymbol{U}^h,\boldsymbol{v}^h,\boldsymbol{\omega}^h)$ be the numerical solution to* (5.3) - (5.4)*. Then we have the consistency error $c^h=\mathcal{L}^h(\boldsymbol{U},\boldsymbol{v},\boldsymbol{\omega})-\mathcal{L}^h(\boldsymbol{U}^h,\boldsymbol{v}^h,\boldsymbol{\omega}^h)$ as*

$$(c^h)_{\boldsymbol{x}_h}=\begin{cases}O(h^2), & \text{if}\quad \boldsymbol{x}_h\in\Omega_\circ^h\\ O(1), & \text{if}\quad \boldsymbol{x}_h\in\Omega_\Gamma^h.\end{cases}\tag{5.8}$$

Proof. We give the proof for $d=2$; the case for $d=3$ is shown in the similar argument. For each cell C_{ij}, the divergence theorem gives

$$0=\int\limits_{C_{ij}\cap\Omega}\nabla\cdot\boldsymbol{U}\,dx=\int\limits_{\partial(C_{ij}\cap\Omega)}\boldsymbol{U}\cdot\boldsymbol{n}\,dS=\int\limits_{\partial C_{ij}\cap\Omega}\boldsymbol{U}\cdot\boldsymbol{n}\,dS+\int\limits_{C_{ij}\cap\Gamma}(\boldsymbol{v}\cdot\boldsymbol{n}+\boldsymbol{\omega}\cdot\boldsymbol{J})\,dS.\tag{5.9}$$

Let $\boldsymbol{U}=(u,v)$. On $\partial C_{ij}\cap\Omega$, we have

$$\begin{aligned}\int\limits_{\partial C_{ij}\cap\Omega}\boldsymbol{U}\cdot\boldsymbol{n}\,dS=&\int\limits_{E_{i+\frac12,j}\cap\Omega}u(x_{i+\frac12},y)\,dy-\int\limits_{E_{i-\frac12,j}\cap\Omega}u(x_{i-\frac12},y)\,dy\\ &+\int\limits_{E_{i,j+\frac12}\cap\Omega}v(x,y_{i+\frac12})\,dx-\int\limits_{E_{i,j-\frac12}\cap\Omega}v(x,y_{i-\frac12})\,dx.\end{aligned}$$

Applying the Taylor series expansion at the middle point of the edge, we estimate the integrals on the right-hand side

$$
\begin{aligned}
\int\limits_{E_{i+\frac{1}{2},j}\cap\Omega} & u(x_{i+\frac{1}{2}},y)\,dy - hH_{i+\frac{1}{2},j}u(x_{i+\frac{1}{2}},y_j) \\
&= \int\limits_{E_{i+\frac{1}{2},j}\cap\Omega} \Big(u(x_{i+\frac{1}{2}},y) - u(x_{i+\frac{1}{2}},y_j)\Big)\,dy \\
&= u_y(x_{i+\frac{1}{2}},y_j) \int\limits_{E_{i+\frac{1}{2},j}\cap\Omega} (y-y_j)\,dy + O(h^3).
\end{aligned}
$$

In particular, if $H_{i\pm\frac{1}{2},j} = 1$, then we have

$$
\int\limits_{E_{i+\frac{1}{2},j}\cap\Omega} u(x_{i+\frac{1}{2}},y)\,dy \;-\int\limits_{E_{i-\frac{1}{2},j}\cap\Omega} u(x_{i+\frac{1}{2}},y)\,dy = h\,u(x_{i+\frac{1}{2}},y_j) - h\,u(x_{i-\frac{1}{2}},y_j) + O(h^4).
$$

We obtain the similar estimations for the other edges. Combining the estimations, we have

$$
\int\limits_{\partial C_{ij}\cap\Omega} \boldsymbol{U}\cdot\boldsymbol{n}\,dS - (\mathrm{D}(H\boldsymbol{U}))_{ij}\,h^2 = \begin{cases} O(h^4) & \text{if } (x_i,y_j)\in\Omega^h_\circ \\ O(h^2) & \text{if } (x_i,y_j)\in\Omega^h_\Gamma. \end{cases} \tag{5.10}
$$

Since $\mathcal{L}^h(\boldsymbol{U}^h,\boldsymbol{v}^h,\boldsymbol{\omega}^h) = 0$, using Lemma 5.1 and Equation (5.9), we have the consistency error $(c^h)_{ij}$ at $(x_i,y_j)\in\Omega^h$ as

$$
\begin{aligned}
h^2(c^h)_{ij} &= h^2\Big(\mathcal{L}^h(\boldsymbol{U},\boldsymbol{v},\boldsymbol{\omega}) - \mathcal{L}^h(\boldsymbol{U}^h,\boldsymbol{v}^h,\boldsymbol{\omega}^h)\Big)_{ij} = h^2\left(\mathcal{L}^h(\boldsymbol{U},\boldsymbol{v},\boldsymbol{\omega})\right)_{ij} \\
&= -h^2(\mathrm{D}(H\boldsymbol{U}))_{ij} + h^2(\mathrm{G}\,H)_{ij}\cdot\boldsymbol{v} + h^2(\boldsymbol{J}^h)_{ij}\cdot\boldsymbol{\omega} \\
&= -h^2(\mathrm{D}(H\boldsymbol{U}))_{ij} - \int_{C_{ij}\cap\Gamma}(\boldsymbol{v}\cdot\boldsymbol{n} + \boldsymbol{\omega}\cdot\boldsymbol{J})\,dS \\
&= \int_{\partial C_{ij}\cap\Omega}\boldsymbol{U}\cdot\boldsymbol{n}\,dS - (\mathrm{D}(H\boldsymbol{U}))_{ij}h^2.
\end{aligned}
$$

Then the estimation (5.10) shows the consistency error (5.8) for $d = 2$.

Now, we consider the case for $d = 3$. A similar argument used for $d = 2$ shows that for each cell C_{ijk}, we have

$$
\int\limits_{\partial C_{ijk}\cap\Omega}\boldsymbol{U}\cdot\boldsymbol{n}\,dS = -\int\limits_{C_{ijk}\cap\Gamma}(\boldsymbol{v}\cdot\boldsymbol{n} + \boldsymbol{\omega}\cdot\boldsymbol{J})\,dS.
$$

and

$$
\int\limits_{\partial C_{ijk}\cap\Omega} \boldsymbol{U}\cdot\boldsymbol{n}\,dS - (\mathrm{D}(H\boldsymbol{U}))_{ijk}\,h^3 = \begin{cases} O(h^5) & \text{if } (x_i,y_j,z_k)\in\Omega^h_\circ \\ O(h^3) & \text{if } (x_i,y_j,z_k)\in\Omega^h_\Gamma. \end{cases} \tag{5.11}
$$

Since $L^h(\boldsymbol{U}^h, \boldsymbol{v}^h, \boldsymbol{\omega}^h) = 0$, we have the consistency error $(c^h)_{ijk}$ at $(x_i, y_j, z_k) \in \Omega^h$ as

$$\begin{aligned} h^3 (c^h)_{ijk} &= h^3 \left(\mathcal{L}^h(\boldsymbol{U}, \boldsymbol{v}, \boldsymbol{\omega}) - \mathcal{L}^h(\boldsymbol{U}^h, \boldsymbol{v}^h, \boldsymbol{\omega}^h) \right)_{ijk} \\ &= -h^3 (\mathrm{D}(H\boldsymbol{U}))_{ijk} + h^3 (\mathrm{G}\, H)_{ijk} \cdot \boldsymbol{v} + h^3 (\boldsymbol{J}^h)_{ijk} \cdot \boldsymbol{\omega} \\ &= -h^3 (\mathrm{D}(H\boldsymbol{U}))_{ijk} - \int\limits_{C_{ijk} \cap \Gamma} (\boldsymbol{v} \cdot \boldsymbol{n} + \boldsymbol{\omega} \cdot \boldsymbol{J}) \; dS + h^3 \boldsymbol{\varepsilon}_{ijk} \cdot \boldsymbol{\omega} \\ &= \int\limits_{\partial C_{ijk} \cap \Omega} \boldsymbol{U} \cdot \boldsymbol{n} \, dS - (\mathrm{D}(H\boldsymbol{U}))_{ijk} \, h^3 + h^3 \boldsymbol{\varepsilon}_{ijk} \cdot \boldsymbol{\omega}. \end{aligned}$$

From (5.5), we see that $|\boldsymbol{\varepsilon}_{ijk}| = O(1)$ if $(x_i, y_j, z_k) \in \Omega^h_\Gamma$ and $\boldsymbol{\varepsilon}_{ijk} = 0$ if $(x_i, y_j, z_k) \in \Omega^h_o$. From the estimation (5.11), we shows the consistency error (5.8) for $d = 3$, which completes the proof. ■

The proof of Theorem 5.1 reveals that there exists a vector field

$$\boldsymbol{d}^h = \begin{cases} (d^h_{i+\frac{1}{2},j}, \; d^h_{i,j+\frac{1}{2}}) & \text{for } d = 2 \\ (d^h_{i+\frac{1}{2},j,k}, \; d^h_{i,j+\frac{1}{2},k}, \; d^h_{i,j,k+\frac{1}{2}}) & \text{for } d = 3 \end{cases}$$

such that for each $\boldsymbol{x}_h \in \Omega^h$

$$h^d \left(\mathrm{D}(H\boldsymbol{d}^h) \right)_{\boldsymbol{x}_h} = h^d \left(\mathcal{L}^h(\boldsymbol{U}, \boldsymbol{v}, \boldsymbol{\omega}) \right)_{\boldsymbol{x}_h}.$$

For example, $d^h_{i+\frac{1}{2},j}$ is given as

$$hH_{i+\frac{1}{2},j} \; d^h_{i+\frac{1}{2},j} = \int\limits_{E_{i+\frac{1}{2},j} \cap \Omega} \left(\boldsymbol{U}(x_{i+\frac{1}{2}}, y) - \boldsymbol{U}(x_{i+\frac{1}{2}}, y_j) \right) \cdot \boldsymbol{n} \, dy$$

and $d^h_{i+\frac{1}{2},j,k}$ is given as

$$\begin{aligned} h^2 H_{i+\frac{1}{2},j,k} \; d^h_{i+\frac{1}{2},j,k} = \int\limits_{F_{i+\frac{1}{2},j,k} \cap \Omega} & \Big\{ \left(\boldsymbol{U}(x_{i+\frac{1}{2}}, y, z) - \boldsymbol{U}(x_{i+\frac{1}{2}}, y_j, z_k) \right) \cdot \boldsymbol{n} \\ & - \left(\omega_2 (z - z_k) - \omega_3 (y - y_j) \right) \Big\} dydz, \end{aligned}$$

where $\boldsymbol{\omega} = (\omega_1, \omega_2, \omega_3)$ and we used the fact from Lemma 2.1 that

$$h^3 \boldsymbol{\varepsilon}_{ijk} \cdot \boldsymbol{\omega} = \boldsymbol{\omega} \cdot \int\limits_{C_{ijk} \cap \Gamma} (\boldsymbol{x} - \boldsymbol{x}_{ijk}) \times \boldsymbol{n} \, dS = -\boldsymbol{\omega} \cdot \int\limits_{\partial C_{ijk} \cap \Omega} (\boldsymbol{x} - \boldsymbol{x}_{ijk}) \times \boldsymbol{n} \, dS.$$

It is not difficult to see that

$$\begin{aligned} d^h_{i+\frac{1}{2},j} &= \begin{cases} O(h) & \text{if} \quad 0 < H_{i+\frac{1}{2},j} < 1 \\ O(h^2) & \text{if} \quad H_{i+\frac{1}{2},j} = 1. \end{cases} \\ d^h_{i+\frac{1}{2},j,k} &= \begin{cases} O(h) & \text{if} \quad 0 < H_{i+\frac{1}{2},j,k} < 1 \\ O(h^2) & \text{if} \quad H_{i+\frac{1}{2},j,k} = 1. \end{cases} \end{aligned} \tag{5.12}$$

and the same holds for $d_{i,j+\frac{1}{2}}$, $d_{i,j+\frac{1}{2},k}$, and $d_{i,j,k+\frac{1}{2}}$.

Note that from the definition of $\boldsymbol{d}^h$, we have

$$\mathcal{L}^h(\boldsymbol{U}-\boldsymbol{U}^h-\boldsymbol{d}^h,\boldsymbol{v}-\boldsymbol{v}^h,\boldsymbol{\omega}-\boldsymbol{\omega}^h)=0.$$

Theorem 5.2 (Convergence error). *Let* $(\boldsymbol{U},\boldsymbol{v},\boldsymbol{\omega})$ *be a continuous solution to* (5.1) - (5.2)*, and* $(\boldsymbol{U}^h,\boldsymbol{v}^h,\boldsymbol{\omega}^h)$ *a numerical solution to* (5.3) - (5.4)*. Then we have the convergence error* $(\boldsymbol{U}_e,\boldsymbol{v}_e,\boldsymbol{\omega}_e):=(\boldsymbol{U}-\boldsymbol{U}^h,\boldsymbol{v}-\boldsymbol{v}^h,\boldsymbol{\omega}-\boldsymbol{\omega}^h)$ *with*

$$\|(\boldsymbol{U}_e,\boldsymbol{v}_e,\boldsymbol{\omega}_e)\|_{E_h}=\left(\frac{1}{2}\int\rho H\boldsymbol{U}_e\cdot\boldsymbol{U}_e\,d\Omega^h+\frac{1}{2}m\boldsymbol{v}_e\cdot\boldsymbol{v}_e+\frac{1}{2}\boldsymbol{\omega}_e\cdot\mathbb{I}\boldsymbol{\omega}_e\right)^{\frac{1}{2}}=O(h).$$

Proof. From the decompositions (5.1) and (5.4), we have

$$\begin{pmatrix}\boldsymbol{U}_e-\boldsymbol{d}^h\\ \boldsymbol{v}_e\\ \boldsymbol{\omega}_e\end{pmatrix}=\begin{pmatrix}\frac{1}{\rho}\operatorname{G}p^h-\frac{1}{\rho}\nabla p-\boldsymbol{d}^h\\ \frac{1}{m}\int(p^h\operatorname{G}H)\,d\Omega^h+\frac{1}{m}\int_\Gamma p\boldsymbol{n}\,dS\\ \mathbb{I}^{-1}\int(p^h\boldsymbol{J}^h)\,d\Omega^h+\mathbb{I}^{-1}\int_\Gamma p\boldsymbol{J}\,dS\end{pmatrix}$$
$$=\begin{pmatrix}\frac{1}{\rho}(\operatorname{G}p^h-\operatorname{G}p)\\ \frac{1}{m}\int(p^h-p)\operatorname{G}H\,d\Omega^h\\ \mathbb{I}^{-1}\int(p^h-p)\boldsymbol{J}^h\,d\Omega^h\end{pmatrix}+\begin{pmatrix}\frac{1}{\rho}\operatorname{G}p-\frac{1}{\rho}\nabla p-\boldsymbol{d}^h\\ \frac{1}{m}\int_\Gamma p\boldsymbol{n}\,dS+\frac{1}{m}\int(p\operatorname{G}H)\,d\Omega^h\\ \mathbb{I}^{-1}\int_\Gamma p\boldsymbol{J}\,dS+\mathbb{I}^{-1}\int p\boldsymbol{J}^h\,d\Omega^h\end{pmatrix}$$

We have shown that $\mathcal{L}^h(\boldsymbol{U}_e-\boldsymbol{d}^h,\boldsymbol{v}_e,\boldsymbol{\omega}_e)=0$. Now we show that $(\boldsymbol{U}_e-\boldsymbol{d}^h,\boldsymbol{v}_e,\boldsymbol{\omega}_e)$ is the projection of $(\boldsymbol{\Lambda}_{\boldsymbol{U}}-\boldsymbol{d}^h,\boldsymbol{\Lambda}_{\boldsymbol{v}},\boldsymbol{\Lambda}_{\boldsymbol{\omega}})$, where

$$\begin{aligned}\boldsymbol{\Lambda}_{\boldsymbol{U}}&:=\frac{1}{\rho}\operatorname{G}p-\frac{1}{\rho}\nabla p,\\ \boldsymbol{\Lambda}_{\boldsymbol{v}}&:=\frac{1}{m}\int_\Gamma p\boldsymbol{n}\,dS+\frac{1}{m}\int p\operatorname{G}H\,d\Omega^h,\\ \boldsymbol{\Lambda}_{\boldsymbol{\omega}}&:=\mathbb{I}^{-1}\int_\Gamma p\boldsymbol{J}\,dS+\mathbb{I}^{-1}\int p\boldsymbol{J}^h\,d\Omega^h,\end{aligned}$$

which follows if we prove that $(\boldsymbol{U}_e-\boldsymbol{d}^h,\boldsymbol{v}_e,\boldsymbol{\omega}_e)$ and

$$\left(\frac{1}{\rho}(\operatorname{G}p^h-\operatorname{G}p),\ \frac{1}{m}\int(p^h-p)\operatorname{G}H\,d\Omega^h,\ \mathbb{I}^{-1}\int(p^h-p)\boldsymbol{J}^h\,d\Omega^h\right)$$

are orthogonal with respect to the inner product $\langle\cdot,\cdot\rangle_{E_h}$. Indeed, the discrete integration by parts yields that their inner product equals

$$\frac{1}{2}\int(-\operatorname{D}H(\boldsymbol{U}_e-\boldsymbol{d}^h)+\boldsymbol{v}_e\cdot\operatorname{G}H+\boldsymbol{\omega}_e\cdot\boldsymbol{J}^h)(p^h-p)\,d\Omega^h$$
$$=\frac{1}{2}\int\mathcal{L}^h(\boldsymbol{U}_e-\boldsymbol{d}^h,\boldsymbol{v}_e,\boldsymbol{\omega}_e)(p^h-p)\,d\Omega^h=0.$$

The orthogonality implies

$$\begin{aligned}\|(\boldsymbol{U}_e,\boldsymbol{v}_e,\boldsymbol{\omega}_e)\|_{E_h}-\|(\boldsymbol{d}^h,0,0)\|_{E_h} &\le \|(\boldsymbol{U}_e-\boldsymbol{d}^h,\boldsymbol{v}_e,\boldsymbol{\omega}_e)\|_{E_h}\\ &\le \|(\boldsymbol{\Lambda_U}-\boldsymbol{d}^h,\boldsymbol{\Lambda_v},\boldsymbol{\Lambda_\omega})\|_{E_h}\\ &\le \|(\boldsymbol{\Lambda_U},\boldsymbol{\Lambda_v},\boldsymbol{\Lambda_\omega})\|_{E_h}+\|(\boldsymbol{d}^h,0,0)\|_{E_h}\end{aligned}$$

The estimation for $\boldsymbol{d}^h$ in (5.12) implies that for $d=2$ we have

$$\begin{aligned}\|(\boldsymbol{d}^h,0,0)\|_{E_h}^2 &= \sum_{i,j}\frac{1}{2}\left(\rho_{i+\frac{1}{2},j}\,H_{i+\frac{1}{2},j}\,(d^h_{i+\frac{1}{2},j})^2+\rho_{i,j+\frac{1}{2}}\,H_{i,j+\frac{1}{2}}\,(d^h_{i,j+\frac{1}{2}})^2\right)h^2\\ &= \sum_{H_{i+\frac{1}{2},j}=H_{i,j+\frac{1}{2}}=1} O(h^4)\,h^2+\sum_{0<H_{i+\frac{1}{2},j},\;H_{i,j+\frac{1}{2}}<1} O(h^2)\,h^2\\ &= O(h^4)+O(h^3)=O(h^3)\end{aligned}$$

and for $d=3$ we similarly have

$$\begin{aligned}\|(\boldsymbol{d}^h,0,0)\|_{E_h}^2 = &\sum_{H_{i+\frac{1}{2},j,k}=H_{i,j+\frac{1}{2},k}=H_{i,j,k+\frac{1}{2}}=1} O(h^4)\,h^3\\ &+\sum_{0<H_{i+\frac{1}{2},j,k},H_{i,j+\frac{1}{2},k},H_{i,j,k+\frac{1}{2}}<1} O(h^2)\,h^3=O(h^4)+O(h^3)=O(h^3).\end{aligned}$$

Here, we used the fact that the number of inside edges, where $H=1$, grows as $O(h^d)$ and that of edges near the boundary, where $0<H<1$, grows as $O(h^{d-1})$.

And Lemma 5.1 (iii) shows

$$m\boldsymbol{\Lambda_v}=\int_\Gamma p\boldsymbol{n}\,dS+\int(p\,\mathrm{G}\,H)\,d\Omega^h=\sum_{\boldsymbol{x}_h\in\Omega_\Gamma^h}\int_{\Gamma\cap C_{\boldsymbol{x}_h}}(p-p_{\boldsymbol{x}_h})\boldsymbol{n}\,dS=O(h)$$

and

$$\mathbb{I}\,\boldsymbol{\Lambda_\omega}=\int_\Gamma p\boldsymbol{J}\,dS+\int p\boldsymbol{J}^h\,d\Omega^h=O(h).$$

On the other hand, the standard central finite difference operator G gives

$$\mathrm{G}\,p-\nabla p=\rho\,\boldsymbol{\Lambda_U}=O(h^2).$$

Combining all the estimations for $\boldsymbol{\Lambda_U}$, $\boldsymbol{\Lambda_v}$, and $\boldsymbol{\Lambda_\omega}$, we conclude that

$$\begin{aligned}\|(\boldsymbol{\Lambda_U},\boldsymbol{\Lambda_v},\boldsymbol{\Lambda_\omega})\|_{E_h}^2 &= \frac{1}{2}\int H(\mathrm{G}\,p-\nabla p)\cdot(\mathrm{G}\,p-\nabla p)\,d\Omega^h\\ &\quad+\frac{1}{2}m\boldsymbol{\Lambda}_v\cdot\boldsymbol{\Lambda}_v+\frac{1}{2}\boldsymbol{\Lambda}_\omega\cdot\mathbb{I}\boldsymbol{\Lambda}_\omega\\ &= O(h^4)+O(h^2)+O(h^2)=O(h^2).\end{aligned}$$

Consequently, we have

$$\begin{aligned}\|(\boldsymbol{U}_e,\boldsymbol{v}_e,\boldsymbol{\omega}_e)\|_{E_h} &\le \|(\boldsymbol{\Lambda_U},\boldsymbol{\Lambda_v},\boldsymbol{\Lambda_\omega})\|_{E_h}+2\|(\boldsymbol{d}^h,0,0)\|_{E_h}\\ &= O(h)+O(h^{1.5})=O(h),\end{aligned}$$

which proves the theorem. ■

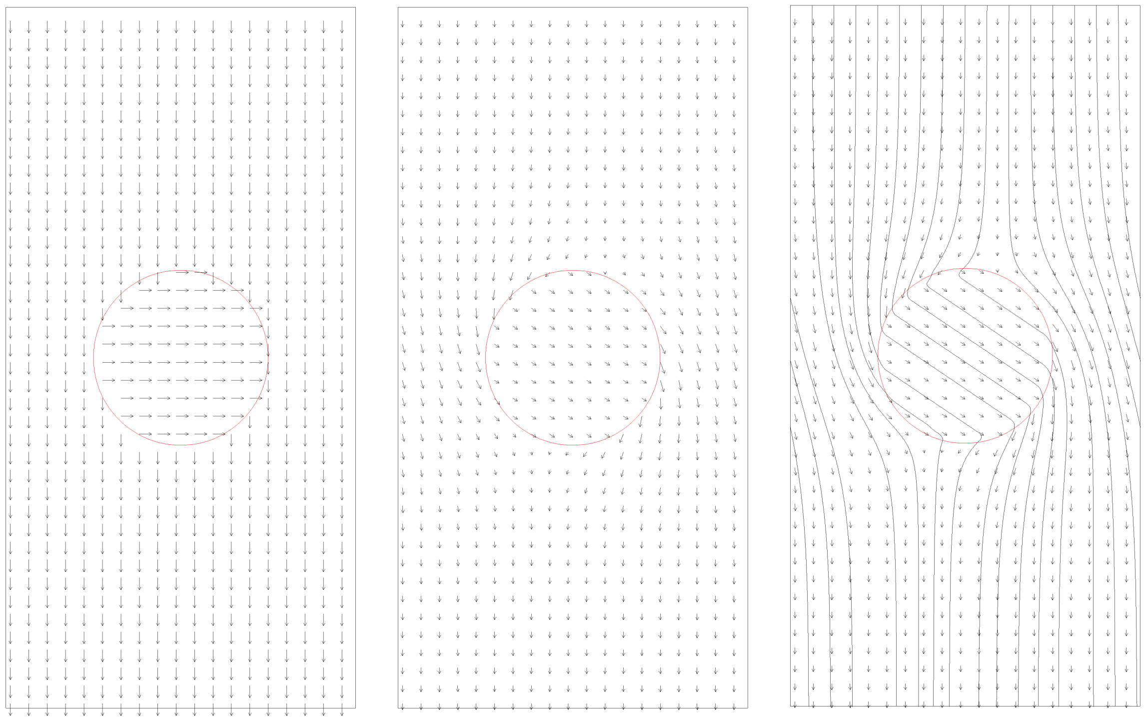

FIGURE 6.1. The velocity fields of fluid and solid before (left) and after (middle) the augmented Hodge projection, and the streamlines (right) after projection.

6. NUMERICAL TEST

6.1. **Orthogonality and stability.** We showed in Theorem 4.3 that the augmented Hodge projection satisfies the orthogonality and the stability, and numerically validate both of the properties in this example. In $[-2,2]\times[-4,4]$, a solid with mass $m=4$ and inertia $\mathbb{I}=2$ is located in a ball centered at $(0,0)$ with radius 1. Fluid with density $\rho=1$ fills the rectangle outside the solid. In this setting, the augmented projection is performed on $\boldsymbol{U}^*=(0,-1)$, $\boldsymbol{v}^*=(\cos\theta,\sin\theta)$, and $\boldsymbol{\omega}^*=0$ for each angle $\theta\in[0,2\pi]$. On the boundary of the rectangle, the periodic boundary condition is imposed to focus on the interface between fluid and solid. Figure 6.1 depicts the velocity fields before and after the projection, and the streamlines in the case $\theta=0$. Note that the velocity fields before the projection does not satisfy the non-penetration condition $\boldsymbol{U}\cdot\boldsymbol{n}=\boldsymbol{U}^{solid}\cdot\boldsymbol{n}$. After the projection, the solid vector field is clearly uniform and the non-penetration condition is now satisfied.

Figure 6.1 validates the theorem that the orthogonality condition

$$\langle(\boldsymbol{U}^h,\boldsymbol{v}^h,\boldsymbol{\omega}^h),(\boldsymbol{U}^*-\boldsymbol{U}^h,\boldsymbol{v}^*-\boldsymbol{v}^h,\boldsymbol{\omega}^*-\boldsymbol{\omega}^h)\rangle_{E_h}=0$$

and the stability condition $\|(\boldsymbol{U}^h,\boldsymbol{v}^h,\boldsymbol{\omega}^h)\|_{E_h}\le\|(\boldsymbol{U}^*,\boldsymbol{v}^*,\boldsymbol{\omega}^*)\|_{E_h}$ are satisfied for all $\theta\in[0,2\pi]$. The numerical solution $(\boldsymbol{U}^h,\boldsymbol{v}^h,\boldsymbol{\omega}^h)$ was computed in a uniform grid 40×80.

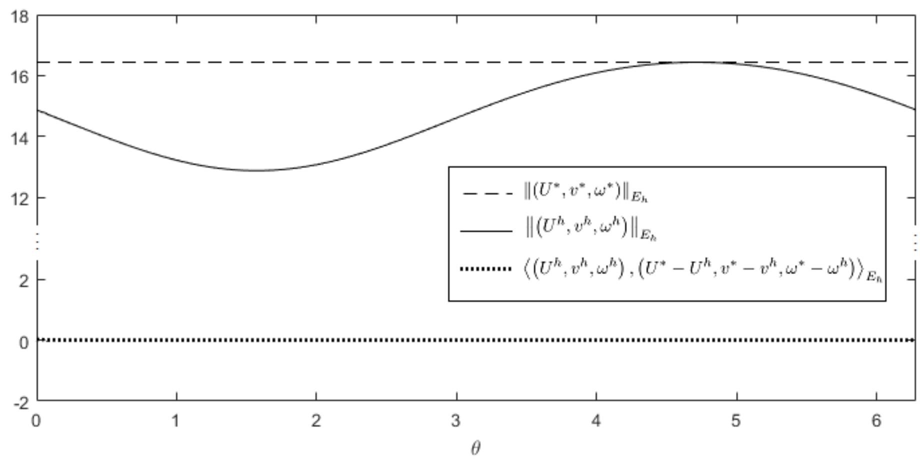

FIGURE 6.2. The kinetic energy before (dashed line) and after (solid line) the augmented Hodge projection, and the inner product. This figure validates $\|(\boldsymbol{U}^h, \boldsymbol{v}^h, \boldsymbol{\omega}^h)\|_{E_h} \le \|(\boldsymbol{U}^*, \boldsymbol{v}^*, \boldsymbol{\omega}^*)\|_{E_h}$ and $\langle(\boldsymbol{U}^h, \boldsymbol{v}^h, \boldsymbol{\omega}^h), (\boldsymbol{U}^* - \boldsymbol{U}^h, \boldsymbol{v}^* - \boldsymbol{v}^h, \boldsymbol{\omega}^* - \boldsymbol{\omega}^h)\rangle_{E_h} = 0$.

6.2. **Convergence in two dimensions.** We showed in Theorem 5.2 that

$$\|(\boldsymbol{U}^h, \boldsymbol{v}^h, \boldsymbol{\omega}^h) - (\boldsymbol{U}, \boldsymbol{v}, \boldsymbol{\omega}\|_{E_h} = O(h),$$

which implies that each of the approximations $\boldsymbol{U}^h \simeq \boldsymbol{U}$, $\boldsymbol{v}^h \simeq \boldsymbol{v}$, and $\boldsymbol{\omega}^h \simeq \boldsymbol{\omega}$ is at least first-order accurate. In this example, we numerically validate the convergence order. Inside $\left[-\frac{\pi}{2}, \frac{\pi}{2}\right]^2$, a solid with mass $m = 1$ and inertia $\mathbb{I} = \mathbb{E}$ is located in a domain $\left\{(x, y) \,|\, \cos x \cos y < \frac{\sqrt{3}}{2}\right\}$. Fluid with density $\rho = 1$ fills the rectangle outside the solid. In this setting, the augmented Hodge projection is performed on $\boldsymbol{U}^* = \boldsymbol{U} + \frac{1}{\rho}\nabla p$, $\boldsymbol{v}^* = 0 - \frac{1}{m}\int_\Gamma p\boldsymbol{n} ds$, and $\boldsymbol{\omega}^* = 0 - \mathbb{I}^{-1}\int_\Gamma p\boldsymbol{J} ds$ with $\boldsymbol{U}(x, y) = (\cos x \sin y, -\sin x \cos y)$ and $p(x, y) = e^{-(x-1)^2 + y}$.

Note that $\boldsymbol{U}$ satisfies the incompressibility condition $\nabla \cdot \boldsymbol{U} = 0$ and the non-penetration condition $\boldsymbol{U} \cdot \boldsymbol{n} = 0$ on the rectangular boundary as well as on the interface $\Gamma = \{(x, y) | \cos x \cos y = \frac{\sqrt{3}}{2}\}$. Numerically computed solutions $(\boldsymbol{U}^h, \boldsymbol{v}^h, \boldsymbol{\omega}^h)$ are compared to the exact solution $(\boldsymbol{U}, \boldsymbol{v} = 0, \boldsymbol{\omega} = 0)$. The exact values of the boundary integrals are

$$\int_\Gamma p\boldsymbol{n}\, dS = [-0.61757657740494\cdots, -0.35222653922478\cdots]$$

and

$$\int_\Gamma p\boldsymbol{J}\, dS = -0.0000757711760965\cdots.$$

Table 1 reports the numerical results. The convergence order of $\|(\boldsymbol{U}^h, \boldsymbol{v}^h, \boldsymbol{\omega}^h) - (\boldsymbol{U}, \boldsymbol{v}, \boldsymbol{\omega})\|_{E_h}$ with respect to h fluctuates, but its least squares fit, as plotted in Figure 6.3, indicates that the convergence order is 1.61. In the following estimate obtained from combining Lemma 5.1 (iii) and the last inequality in the proof of Theorem 5.2,

$$\|(\boldsymbol{U} - \boldsymbol{U}^h, \boldsymbol{v} - \boldsymbol{v}^h, \boldsymbol{\omega} - \boldsymbol{\omega}^h)\|_{E_h} \le \frac{|\Gamma|\,((\operatorname{diam}\Gamma) + 1)\,\|\nabla p\|_{L^\infty}}{2}\, h + O(h^{1.5}),$$

grid	h	$\|(\boldsymbol{U}-\boldsymbol{U}^h, \boldsymbol{v}-\boldsymbol{v}^h, \boldsymbol{\omega}-\boldsymbol{\omega}^h)\|_{E_h}$	order
20^2	$\frac{\pi}{20}$	3.14×10^{-2}	
40^2	$\frac{\pi}{40}$	5.01×10^{-3}	2.65
80^2	$\frac{\pi}{80}$	3.42×10^{-3}	0.551
160^2	$\frac{\pi}{160}$	5.70×10^{-4}	2.58
320^2	$\frac{\pi}{320}$	4.17×10^{-4}	0.451
640^2	$\frac{\pi}{640}$	6.99×10^{-5}	2.57

TABLE 1. Convergence order in the example of two dimensions. The order fluctuates, and its least squares fitting is tried in Figure 6.3.

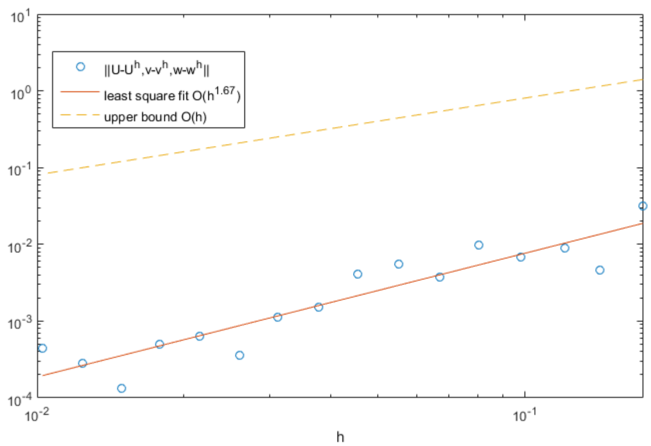

FIGURE 6.3. Log-plot of the least squares fit of the errors $\|\left(\boldsymbol{U}^h, \boldsymbol{v}^h, \boldsymbol{\omega}^h\right) - (\boldsymbol{U}, \boldsymbol{v}, \boldsymbol{\omega})\|_{E_h}$ in the example of two dimensions. The errors are certainly below the upper bound $O(h)$.

Individual error	order
$\|\boldsymbol{U}-\boldsymbol{U}^h\|_{L^2}$	$O(h^{1.61})$
$\|\boldsymbol{v}-\boldsymbol{v}^h\|$	$O(h^{1.73})$
$\|\boldsymbol{\omega}-\boldsymbol{\omega}^h\|$	$O(h^{2.72})$

TABLE 2. The convergence order of each individual error in the sum $\|\left(\boldsymbol{U}^h, \boldsymbol{v}^h, \boldsymbol{\omega}^h\right) - (\boldsymbol{U}, \boldsymbol{v}, \boldsymbol{\omega})\|_{E_h}^2 = \frac{\rho}{2}\|\boldsymbol{U}^h - \boldsymbol{U}\|_{L^2}^2 + \frac{m}{2}\|\boldsymbol{v}^h - \boldsymbol{v}\|^2 + \frac{\mathbb{I}}{2}\|\boldsymbol{\omega}^h - \boldsymbol{\omega}\|^2$. For the same data in Figure 6.3, the order was obtained from the least squares fit of each error.

the first term becomes dominant and forms an upper bound of the error for sufficiently small h. All the errors in Figure 6.3 are certainly below the upper bound, which validates the theorem. We deduced from the theorem that each of $\boldsymbol{U}^h \simeq \boldsymbol{U}, \boldsymbol{v}^h \simeq v, \boldsymbol{\omega}^h \simeq \boldsymbol{\omega}$ is at least first order accurate. Table 2 confirms the deduction.

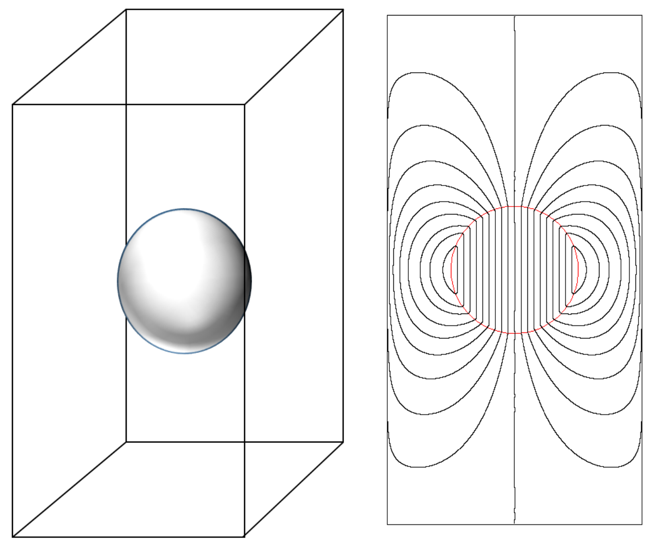

FIGURE 6.4. The physical setting for the example of three dimensions (left) and the streamlines after the projection in section $x = 0$ (right).

grid	h	$\|(\boldsymbol{U}^{2h}, \boldsymbol{v}^{2h}, \boldsymbol{\omega}^{2h}) - (\boldsymbol{U}^h, \boldsymbol{v}^h, \boldsymbol{\omega}^h)\|_{E_h}$	order
$16^2 \times 32$	$\frac{1}{4}$	6.16×10^{-2}	
$32^2 \times 64$	$\frac{1}{8}$	1.62×10^{-2}	1.92
$64^2 \times 128$	$\frac{1}{16}$	4.31×10^{-3}	1.91
$128^2 \times 256$	$\frac{1}{32}$	1.26×10^{-3}	1.77
$256^2 \times 512$	$\frac{1}{64}$	3.74×10^{-4}	1.75

TABLE 3. The convergence error in the example of three dimensions

6.3. **Convergence in three dimensions.** We measure the convergence order of the discrete Hodge projection in a three-dimensional example. In $[-2, 2]^2 \times [-4, 4]$, a solid with mass $m = \frac{8}{3}\pi$ and inertia $\mathbb{I} = \frac{16}{15}\pi\,\mathbb{E}$ is located in a ball centered at $(0, 0, 0)$ of radius one. We recall that $\mathbb{E}$ is the 3×3 identity matrix. Fluid with density $\rho = 1$ fills the box outside the solid. In this setting, the augmented Hodge projection is performed on $\boldsymbol{U}^* = (0, 0, -1)$, $\boldsymbol{v}^* = (0, 0, -1)$, and $\boldsymbol{\omega}^* = (0, 0, 0)$. The non-penetration condition is imposed on the rectangular boundary. Figure 6.4 illustrates the setting.

Since the exact solution is unknown, we instead measure the convergence order through $\|(\boldsymbol{U}^{2h} - \boldsymbol{U}^h, \boldsymbol{v}^{2h} - \boldsymbol{v}^h, \boldsymbol{\omega}^{2h} - \boldsymbol{\omega}^h)\|_{E_h}$, based on the fact that we have

$$\begin{aligned}\|(\boldsymbol{U}^{2h} - \boldsymbol{U}^h, \boldsymbol{v}^{2h} - \boldsymbol{v}^h, \boldsymbol{\omega}^{2h} - \boldsymbol{\omega}^h)\|_{E_h} &\le \|(\boldsymbol{U} - \boldsymbol{U}^{2h}, \boldsymbol{v} - \boldsymbol{v}^{2h}, \boldsymbol{\omega} - \boldsymbol{\omega}^{2h})\|_{E_h} \\ &\quad + \|(\boldsymbol{U} - \boldsymbol{U}^h, \boldsymbol{v} - \boldsymbol{v}^h, \boldsymbol{\omega} - \boldsymbol{\omega}^h)\|_{E_h} \\ &= O(h^\alpha + 2^\alpha h^\alpha) = O(h^\alpha),\end{aligned}$$

whenever $\|(\boldsymbol{U} - \boldsymbol{U}^h, \boldsymbol{v} - \boldsymbol{v}^h, \boldsymbol{\omega} - \boldsymbol{\omega}^h)\|_{E_h} = O(h^\alpha)$ for the exact solution $(\boldsymbol{U}, \boldsymbol{v}, \boldsymbol{\omega})$.

grid	h	$\|\boldsymbol{U}^{2h}-\boldsymbol{U}^h\|_{L^2}$	order	$\|\boldsymbol{v}^h-\boldsymbol{v}^{2h}\|+\|\boldsymbol{\omega}^h-\boldsymbol{\omega}^{2h}\|$	order
$16^2\times 32$	$\frac{1}{4}$	2.65×10^{-2}		5.56×10^{-2}	
$32^2\times 64$	$\frac{1}{8}$	8.74×10^{-3}	1.60	1.36×10^{-2}	2.03
$64^2\times 128$	$\frac{1}{16}$	2.61×10^{-3}	1.74	3.43×10^{-3}	1.98
$128^2\times 256$	$\frac{1}{32}$	9.30×10^{-4}	1.48	8.62×10^{-4}	1.99
$256^2\times 512$	$\frac{1}{64}$	3.50×10^{-4}	1.60	2.16×10^{-4}	2.00

TABLE 4. The convergence errors of $\|\boldsymbol{U}^{2h}-\boldsymbol{U}^h\|_{L^2}$ and $|\boldsymbol{v}^h-\boldsymbol{v}^{2h}|+|\boldsymbol{\omega}^h-\boldsymbol{\omega}^{2h}|$ in the example of three dimensions

Table 3 reports the numerical results, which validates the convergence order $O(h)$ shown in Theorem 5.2. Also the table shows that the order is actually far greater than one. Table 4 indicates that $\|\boldsymbol{U}^{2h}-\boldsymbol{U}^h\|_{L^2}=O(h^{1.6})$ and $|\boldsymbol{v}^h-\boldsymbol{v}^{2h}|+|\boldsymbol{\omega}^h-\boldsymbol{\omega}^{2h}|=O(h^2)$. The convergence error $\|(\boldsymbol{U}^{2h},\boldsymbol{v}^{2h},\boldsymbol{\omega}^{2h})-(\boldsymbol{U}^h,\boldsymbol{v}^h,\boldsymbol{\omega}^h)\|_{E_h}$ can be regarded as a sum of $\|\boldsymbol{U}^{2h}-\boldsymbol{U}^h\|_{L^2}$ and $|\boldsymbol{v}^h-\boldsymbol{v}^{2h}|+|\boldsymbol{\omega}^h-\boldsymbol{\omega}^{2h}|$, when the order calculation is a matter of interests. It implies that $\|(\boldsymbol{U}^{2h},\boldsymbol{v}^{2h},\boldsymbol{\omega}^{2h})-(\boldsymbol{U}^h,\boldsymbol{v}^h,\boldsymbol{\omega}^h)\|_{E_h}$ is mainly influenced by $\|\boldsymbol{U}^{2h}-\boldsymbol{U}^h\|_{L^2}=O(h^{1.6})$ rather than by the other term, when h becomes smaller. This explains why the convergence order in Table 3 slowly decreases toward 1.6.

7. Conclusion and comment

In this work, we have studied a Fluid-Solid interaction by taking a monolithic treatment on fluid-solid interaction. It is based on the fact that fluid velocity field $\boldsymbol{U}$ and solid velocities $\boldsymbol{v}$ and $\boldsymbol{\omega}$ do not separately proceed but as a whole by a combined state variable $(\boldsymbol{U},\boldsymbol{v},\boldsymbol{\omega})$. We introduced the so-called augmented Hodge decomposition of the state variable into two orthogonal components, which is a variation of the Hodge decomposition. The decomposition enables us to decouple the computations of the velocity and the pressure in the incompressible Navier-Stokes equation. Then, the decomposition is fulfilled by solving an elliptic equation for the pressure with non-local Robin type boundary condition. We have shown the existence, uniqueness and the regularity of the solution to the equation. The monolithic treatment leads to the stability that the kinetic energy does not increase in the projection step. Using an Heaviside function, we expressed the boundary condition independent of the interface. We proposed a numerical method producing the numerical solution at least with first order accuracy. Also, we showed that the unique decomposition and orthogonality also hold in the discrete setting. We carried out numerical experiments for 2 and 3 dimensions and the numerical tests validate our analysis and arguments. Even though the experiments supports our arguments, $\|(\boldsymbol{U}^h,\boldsymbol{v}^h,\boldsymbol{\omega}^h)-(\boldsymbol{U},\boldsymbol{v},\boldsymbol{\omega})\|_{E_h}=O(h)$, it reveals that the convergence order is greater than one and the error is mainly influenced by $\|\boldsymbol{U}^{2h}-\boldsymbol{U}^h\|_{L^2}=O(h^{1.6})$ rather than by the other term, when h becomes smaller. The analysis for the phenomenon would involve very different arguments from the current one, and we put it off to future work.

References

[1] S. Badia, F. Nobile, and C. Vergara, *Robin-Robin preconditioned Krylov methods for fluid-structure interaction problems*, Comput. Methods Appl. Mech. Eng., 198, 2768–2784, 2009.

[2] S. Badia, A. Quaini, and A. Quarteroni, *Modular vs. non-modular preconditioners for fluid?structure systems with large addedmass effect*, Comput. Methods Appl. Mech. Eng., 197, 4216–4232, 2008.

[3] C. Batty, F. Bertails, and R. Bridson, *A fast variational framework for accurate solid-fluid coupling*, ACM Trans. Graph. (SIGGRAPH Proc.), 26(3), 2007.

[4] J. B. Bell, P. Colella, and H. M. Glaz, *A second order projection method for the incompressible Navier-Stokes equations*, J. Comput. Phys., 85, 257–283, 1989.

[5] I. Borazjani, L. Ge, and F. Sotiropoulos, *Curvilinear immersed boundary method for simulating fluid structure interaction with complex 3D rigid bodies*, J. Comput. Phys. 227(16), 7587–7620, 2008.

[6] R. Bridson, *Fluid simulation for computer graphics*, A K Pters, Ltd., 2008, 888 Worcester Street, Wellesley, MA 02482.

[7] D. Brown, R. Cortez, and M. Minion, *Accurate projection methods for the incompressible Navier-Stokes equations*, J. Comput. Phys., 168, 464–499, 2001.

[8] M. Bukač, I. Yotov, and P. Zunino, *An operator splitting approach for the interaction between a fluid and a multilayered poroelastic structure*, Numerical Methods for Partial Differential Equations, 31, 1054–1100, 2015.

[9] P. Causin, J. Gerbeau, and F. Nobile, *Added-mass effect in the design of partitioned algorithms for fluid-structure problems*, Comput. Methods Appl. Mech. Eng., 194, 42–44, 2005.

[10] S. K. Chakrabarti (Ed.), *Numerical Models in Fluid Structure Interaction*, Advances in Fluid Mechanics, 42, WIT Press, 2005.

[11] Z. Q. Chen, R. J. Williams, and Z. Zhao, *A Sobolev inequality and Neumann heat kernel estimate for unbounded domains*, Math. Res. Lett., 1, 177–184, 1994.

[12] A. Chorin, *A numerical method for solving incompressible viscous flow problems*, J. Comput. Phys., 2, 12–26, 1967.

[13] J. Degroote, P. Bruggeman, R. Haelterman, and J. Vierendeels, *Stability of a coupling technique for partitioned solvers in FSI applications*, Comput. Struct., 86, 2224–2234, 2008.

[14] E. H. Dowell and K. C. Hall, *Modeling of fluid-structure interaction*, Annual Review of Fluid Mechanics, 33, 445–490, 2001.

[15] L. C. Evans, *Partial differential equations*, Graduate Studies in Mathematics, vol., 19, Amer. Math. Soc., 1998.

[16] C. Farhat, K. van der Zee,and P. Geuzaine, *Provably second-order time-accurate loosely-coupled solution algorithms for transient nonlinear computational aeroelasticity*, Comput. Methods Appl. Mech. Eng., 195, 1973–2001, 2006.

[17] M. Fernández, *Incremental displacement-correction schemes for incompressible fluid-structure interaction*, Numerische Mathematik, 123, 21–65, 2013

[18] M. Fernández and J. Mullaert, *Convergence and error analysis for a class of splitting schemes in incompressible fluid-structure interaction*, IMA Journal of Numerical Analysis, (2015), p. drv055.

[19] C. Förster, W. A. Wall, and E. Ramm, *Artificial added mass instabilities in sequential staggered coupling of nonlinear structures and incompressible viscous flows*, Comput. Methods Appl. Mech. Eng., 196(7), 1278–1293, 2007.

[20] M. Gee, U. Küttler, and W. Wall, *Truly monolithic algebraic multigrid for fluid-structure interaction*, Int. J. Numer. Meth. Eng., 85, 987–1016, 2011.

[21] F. Gibou, R. Fedkiw, L.-T. Cheng, and M. Kang, *A second-order-accurate symmetric discretization of the Poisson equation on irregular domains*, J. Comput. Phys., 176, 205–227, 2002.

[22] F. Gibou and C. Min, *Efficient symmetric positive definite second-order accurate monolithic solver for fluid/solid interactions*, J. Comput. Phys., 231, 3245–3263, 2012.

[23] D. Gilbarg and N. S. Trudinger, *Elliptic partial differential equations of second order*, Reprint of the 1998 ed. Springer-Verlag, Berlin, 2001.

[24] J. T. Grétarsson, N. Kwatra, and R. Fedkiw, *Numerically stable fluid-structure interactions between compressible flow and solid structures*, J. Comput. Phys., 230, 3062–3084, 2011.

[25] J. L. Guermond, P. Minev, and J. Shen, *An overview of projection methods for incompressible flows*, Comput. Methods Appl. Mech. Engrg., 195, 6011?6045, 2006

[26] F. Harlow and J. Welch, *Numerical calculation of time-dependent viscous incompressible flow of fluids with free surfaces*, Physics of Fluids, 8, 2182–2189, 1965.

[27] M. Heil, A. Hazel, and J. Boyle, *Solvers for large-displacement fluid-structure interaction problems: segregated versus monolithic approaches*, Comput. Mech., 43, 91–101, 2008.

[28] H. Helmholtz, *On integrals of the hydrodynamic equations which correspond to vortex motions*, Journal fur die reine und angewandte Mathematik, 55, 25–55, 1858.

[29] B. Hübner, E. Walhorn, and D. Dinkler, *A monolithic approach to fluid-structure interaction using space-time finite elements*, Comput. Methods Appl. Mech. Eng., 193, 2087–2104, 2004.

[30] J. Kim and P. Moin, *Application of a fractional-step method to incompressible Navier-Stokes equations*, J. Comput. Phys., 59, 308–323, 1985.

[31] E. W. Liu and J. G. Liu, *Gauge method for viscous incompressible flows*, Comm. Math. Sci., 1, 317–332, 2003.
[32] C. Michler, S. J. Hulshoff, E. H. van Brummelen, and R. de Borst, *A monolithic approach to fluid-structure interaction*, Comput. Fluids, 33, 839–848, 2004
[33] C. Min and G. Yoon, *Convergence analysis on Gibou-Min method for the scalar field in Hodge-Helmholtz decomposition*, J. Korean Soc. Ind. Appl. Math., 18, 305–316, 2014.
[34] H. J.-P. Morand and R. Ohayon, *Fluid-Structure Interaction: Applied Numerical Methods*, Wiley, 1995.
[35] B. Muha and S. Čanić, *Existence of a Weak Solution to a Nonlinear Fluid-Structure Interaction Problem Modeling the Flow of an Incompressible, Viscous Fluid in a Cylinder with Deformable Walls*, Arch. Rational Mech. Anal., 207, 919–968, 2013.
[36] Y. T. Ng, C. Min, and F. Gibou, *An efficient fluid-solid coupling algorithm for single-phase flows*, J. Comput. Phys., 228, 8807–8829, 2009.
[37] F. Nobile and C. Vergara, *An effective fluid-structure interaction formulation for vascular dynamics by generalized Robin conditions*, SIAM J. Sci. Comput., 30, 731–763, 2008.
[38] C. Pozrikidis, *Introduction to theoretical and computational fluid dynamics*, Oxford university press, 1997.
[39] J. W. Purvis and J. E. Burkhalter, *Prediction of critical Mach number for store configurations*, AIAA J., 17, 1170–1177, 1979.
[40] P. B. Ryzhakov, R. Rossi, S. R. Idelsohn, and E. Oñate, *A monolithic Lagrangian approach for fluid-structure interaction problems*, Comput. Mech., 46, 883–899, 2010.
[41] M. Uhlmann, *An immersed boundary method with direct forcing for the simulation of particulate flows*, J. Comput. Phys., 209(2), 448–476, 2005.
[42] E. Walhorn, A. Kölke, B. Hübner, and D. Dinkler, *Fluid-structure coupling within a monolithic model involving free surface flows*, Comput. Struct., 83, 2100–2111, 2005.
[43] D. Xiu and G. Karniadakis, *A semi-Lagrangian high-order method for Navier-Stokes equations*, J. Comput. Phys., 172, 658–684, 2001.
[44] G. Yoon and C. Min, *Analyses on the finite difference method by Gibou et al. for Poisson equation*, J. Comput. Phys., 280, 184–194, 2015.
[45] G. Yoon and C. Min, *Convergence analysis of the standard central finite difference method for Poisson equation*, J. Sci. Comput., accepted.
[46] G. Yoon, J.-H. Park, and C. Min, *Convergence analysis on the Gibou-Min method for the Hodge projection*, Commun. Math. Sci., submitted.

National Institute for Mathematical Sciences, Daejeon 34047, Korea
E-mail address: yoon@nims.re.kr

Department of Mathematics, Ewha Woman's University, Seoul 03760, Korea
E-mail address: chohong@ewha.ac.kr

Department of Mathematics, Yonsei University, Seoul 03722, Korea
E-mail address: kimseick@yonsei.ac.kr